

RESEARCH

Open Access



# Soil properties drive nitrous oxide accumulation patterns by shaping denitrifying bacteriomes

Saira Bano<sup>1</sup>, Qiaoyu Wu<sup>1</sup>, Siyu Yu<sup>1</sup>, Xinhui Wang<sup>1</sup> and Xiaojun Zhang<sup>1\*</sup>

## Abstract

In agroecosystems, nitrous oxide (N<sub>2</sub>O) emissions are influenced by both microbiome composition and soil properties, yet the relative importance of these factors in determining differential N<sub>2</sub>O emissions remains unclear. This study investigates the impacts of these factors on N<sub>2</sub>O emissions using two primary agricultural soils from northern China: fluvo-aquic soil (FS) from the North China Plain and black soil (BS) from Northeast China, which exhibit significant differences in physicochemical properties. In non-sterilized controls (NSC), we observed distinct denitrifying bacterial phenotypes between FS and BS, with BS exhibiting significantly higher N<sub>2</sub>O emissions. Cross-inoculation experiments were conducted by introducing extracted microbiomes into sterile recipient soils of both types to disentangle the relative contributions of soil properties and microbiomes on N<sub>2</sub>O emission potential. The results showed recipient-soil-dependent gas kinetics, with significantly higher N<sub>2</sub>O/(N<sub>2</sub>O + N<sub>2</sub>) ratios in BS compared to FS, regardless of the inoculum type. Metagenomic analysis further revealed significant shifts in denitrification genes and microbial diversity of the inoculated bacteriomes influenced by the recipient soil. The higher ratios of *nirS/nosZ* in FS and *nirK/nosZ* in BS indicated that the recipient soil dictates the formation of different denitrifying guilds. Specifically, the BS environment fosters *nirK*-based denitrifiers like *Rhodanobacter*, contributing to higher N<sub>2</sub>O accumulation, while FS supports a diverse array of denitrifiers, including *Pseudomonas* and *Stutzerimonas*, associated with complete denitrification and lower N<sub>2</sub>O emissions. This study underscores the critical role of soil properties in shaping microbial community dynamics and greenhouse gas emissions. These findings highlight the importance of considering soil physicochemical properties in managing agricultural practices to mitigate N<sub>2</sub>O emissions.

**Keywords** Soil properties, Nitrous oxide, Denitrification, Denitrifying bacteria, Denitrifying genes

\*Correspondence:

Xiaojun Zhang  
xjzhang68@sjtu.edu.cn

<sup>1</sup>State Key Laboratory of Microbial metabolism, Joint International Research Laboratory of Metabolic & Developmental Sciences, School of Life Sciences & Biotechnology, Shanghai Jiao Tong University, 800 Dongchuan Road, Minhang District, Shanghai 200240, China



© The Author(s) 2024. **Open Access** This article is licensed under a Creative Commons Attribution 4.0 International License, which permits use, sharing, adaptation, distribution and reproduction in any medium or format, as long as you give appropriate credit to the original author(s) and the source, provide a link to the Creative Commons licence, and indicate if changes were made. The images or other third party material in this article are included in the article's Creative Commons licence, unless indicated otherwise in a credit line to the material. If material is not included in the article's Creative Commons licence and your intended use is not permitted by statutory regulation or exceeds the permitted use, you will need to obtain permission directly from the copyright holder. To view a copy of this licence, visit <http://creativecommons.org/licenses/by/4.0/>.

## Introduction

Nitrous oxide (N<sub>2</sub>O) is a long-lived stratospheric ozone-depleting potent greenhouse gas with a current atmospheric lifetime of 116±9 years [1]. According to the latest IPCC assessment report, over a 100-year time scale, the global warming potential of N<sub>2</sub>O is estimated to be 273 times greater than that of CO<sub>2</sub> [2]. Agroecosystems are significant contributors globally, representing 60% of anthropogenic global N<sub>2</sub>O emissions [3], primarily produced from microbially mediated processes such as denitrification [4].

Denitrification is a microbially mediated process that typically occurs under anoxic conditions when nitrate (NO<sub>3</sub><sup>-</sup>) or nitrite (NO<sub>2</sub><sup>-</sup>) is used as a terminal electron acceptor and reduced to nitrogen (N) gases (dinitrogen (N<sub>2</sub>) and N<sub>2</sub>O) [5]. Complete denitrification is the stepwise reduction of NO<sub>3</sub><sup>-</sup> to N<sub>2</sub>, catalyzed by a series of complex metalloenzymes encoded by genes such as *narG* (NO<sub>3</sub><sup>-</sup> reductase), *nirK* (copper-containing NO<sub>2</sub><sup>-</sup> reductase), *nirS* (cytochrome cd-containing NO<sub>2</sub><sup>-</sup> reductase), *norB* (nitric oxide (NO) reductase), and *nosZ* (N<sub>2</sub>O reductase) [6]. True denitrifiers inherit a complete set of denitrification functional genes and are considered key players in the process [7]. However, the process is usually affected by the diversity and abundance of the denitrifying microbial community [8, 9], as organisms lacking one or more of these genes are called truncated or incomplete denitrifiers and can contribute to significant N<sub>2</sub>O emissions [6, 7].

To date, in agroecosystems, studies have often explained N<sub>2</sub>O fluxes based on either the abundance and diversity of denitrifying microbial communities [9, 10] or variations in soil physicochemical properties [3, 7, 11–15]. Despite advancements in understanding the proximal (microbial) and distal (soil properties) controls influencing N<sub>2</sub>O emissions, the relative contributions of soil properties and microbial community dynamics remain unclear. Soil types, with their distinct physicochemical characteristics such as pH [12], moisture content [13], and nutrient availability [3, 7] can play a pivotal role in shaping microbial community structure and function [16, 17]. For example, when pH value was lower than 6 the activity of nitrous oxide reductase enzyme would be ultimately constrained, resulting in more N<sub>2</sub>O emissions [12]. Similarly, fertilizer-induced changes in soil pH and organic matter attributes reshape distinct denitrifying guilds and ultimately affect N<sub>2</sub>O emissions [18, 19].

According to FAOSTAT (2014), China, despite having only 7% of the world's arable land, produces enough food to feed 19% of the global population [20]. To achieve this, chemical fertilizers are heavily used to boost grain yields, often applied at levels exceeding the optimal requirements [7]. The North China Plain and Northeast China are key agricultural regions, known for large-scale wheat

and corn cultivation, respectively [21, 22]. Overfertilization is a prevalent issue in these areas, with conventional practices applying 550 to 600 kg of N per hectare, far above recommended levels [23], which has led to significant NO<sub>x</sub> emissions [24] and making the region a major contributor to global N<sub>2</sub>O emissions [1]. In North-east China, soils are characterized by low pH and are rich in organic matter, such as black soil, whereas the North China Plain is dominated by alkaline, calcareous fluvo-aquic soils that are low in carbon content [21, 25]. These soil types are markedly different in physicochemical properties and also the soil microbiomes [9], which likely affect the denitrification potential and N<sub>2</sub>O emission rates of these soils differently. This underscores the necessity to dissect the interplay between soil properties and microbial community dynamics to develop effective strategies for mitigating N<sub>2</sub>O emissions.

Effective management of N<sub>2</sub>O emissions from agricultural soils requires an integrated approach that accounts for both microbial community composition and soil physicochemical properties [26, 27]. This study aims to elucidate the interactions between soil properties and microbial community dynamics, emphasizing their functional outcomes regarding N<sub>2</sub>O emissions. Molecular approaches, particularly metagenomic analyses, offer a comprehensive method for tracking shifts in microbial abundance and diversity. They also enable the identification of key functional genes and taxa involved in denitrification processes, providing insights into the mechanisms that drive N<sub>2</sub>O production and reduction in soils [28, 29].

Our hypothesis posits that soil properties act as distal drivers by shaping the selection of microbial communities—the proximal drivers of N<sub>2</sub>O emissions—within the soil environment. This determinism suggests that specific soil environments favour the selection and persistence of microbiomes with particular functional capabilities, reflecting adaptation to the unique conditions of each soil. To test this hypothesis, we conducted extracted-microbiome-based cross-inoculation experiments between fluvo-aquic soil (FS) and black soil (BS). Sterile soils were inoculated with extracted microbiomes originating from either their native soil type or from the other soil type. Using particle-free microbial cell-extraction technology, we prepared microbiome inoculums by separating microbial cells from soil particles. We examined the patterns of N<sub>2</sub>O emission kinetics across the treatments and analysed shifts in the structure of the total bacterial and denitrifying bacterial communities, as well as the relative and absolute abundances of key denitrifying genes. This experimental design enables us to disentangle the contributions of soil properties and inoculated microbiomes to the denitrifying bacterial communities and their N<sub>2</sub>O emission potential. Understanding these

dynamics is essential for developing targeted strategies to mitigate N<sub>2</sub>O emissions in agricultural systems.

## Materials and methods

### Soil sample collection and preparation

Two distinct types of soil samples, FS from the North China Plain and BS from Northeast China, were collected from cropland in long-term experimental fields (Table S1), as detailed by Wu et al. [9]. For each soil type, samples were taken from five different points at depths of 0 to 20 cm and then mixed to create a composite sample. The soil samples were sieved through a 2 mm mesh and placed in black plastic bags. Before incubation experiments, a portion of each soil type was sterilized using gamma irradiation (36 kGy) and stored in closed plastic bags. All samples were kept at 4 °C until use.

Soil pH, NO<sub>3</sub><sup>-</sup>-N, NO<sub>2</sub><sup>-</sup>-N, ammonium (NH<sub>4</sub><sup>+</sup>), and soil moisture content were measured as described previously [9]. Water holding capacity (WHC) was determined using the funnel method, following the procedure outlined in Govindasamy et al. [30] with some modifications (see [supplementary material](#) for details). The soils were preconditioned in the dark at 50% WHC and 25 °C for 7 days before the incubation experiment.

### Microbial cell extraction from the soil

The microbial cell extraction method was adapted from previous literatures [31, 32] with some modifications. Briefly, 20 g (dry weight) of soil sample for each replicate was taken separately in a 150 mL conical flask, pre-activated for one week at 25 °C, and made into 1:5 slurries with sterile water. Each technical replicate was vortexed for 1 min and then aliquoted into a Waring laboratory blender, where it was blended at full speed for five 1-minute intervals with intermittent cooling on ice. The dispersed soil suspensions were set aside for 30 min to allow the coarse soil particles to settle.

A density gradient was created by transferring the soil suspensions into centrifuge tubes and carefully placing an 80% nycodenz (Nycodenz, Oslo, Norway) solution underneath the soil suspension in a 3:1 volume ratio (soil suspension: nycodenz). The tubes were then centrifuged in a high-speed swing-out rotor centrifuge at 4 °C and 14,000×g for 60 min. The middle layer of cells was carefully collected along with some nycodenz solution, excluding the pellet, and transferred into new tubes. These were diluted with sterile water and centrifuged at 14,000×g for 45 min. After discarding the supernatant, the pellet was resuspended in an appropriate amount of sterile water to adjust the WHC of the 20 g of sterilized recipient soil to 50%. The suspension was stored at 4 °C before inoculation. The extracted cells were counted based on the method described by Highton et al. [33].

### Experimental design for the microbial inoculation and anoxic incubation

Two types of soil samples, FS and BS, were arranged into three treatment groups: NSC (pre-activated non-sterilized control), FSB (sterilized soil inoculated with microbial inoculum extracted from pre-activated fluvo-aquic soil), and BSB (sterilized soil inoculated with microbial inoculum extracted from pre-activated black soil) (Fig. S1). Each treatment group included triplicate samples of 20 g (dry weight) of the respective soil, placed in 120 mL serum vials, with 50% WHC and adjusted to initial NO<sub>3</sub><sup>-</sup> (KNO<sub>3</sub>) and carbon (C<sub>6</sub>H<sub>12</sub>O<sub>6</sub>) contents of 250 mg/kg and 1000 mg/kg of soil, respectively.

To compare gas kinetics between the cell extracts and the parent soils, sterile sister soils (gamma-sterilized parent soils) were used for inoculating the cell extracts. This approach was necessary because the cell suspension alone could not fully replicate the soil matrix's effects, particularly regarding gas diffusion and microbial niches. For each replicate, a particle-free cell extract extracted from 20 g of soil was inoculated into 20 g of sterile soil, which served as the extracted cell group for comparison with the 20 g of parent soil during gas kinetics measurement.

The sample vials were sealed with airtight butyl-rubber septa and aluminum crimp caps. Each replicate was inoculated with microbial cells extracted from 20 g (dry weight) of the respective soil, injected into the sealed vials via syringe through the rubber septa. Negative controls of sterile soils (without inoculation) were also prepared to confirm the sterility of the soils. The headspace of the serum vials was alternately evacuated and refilled with high-purity helium (99.999%) four times to create a completely anoxic environment. All vials were incubated at 25 °C, and the headspace was sampled every 6 h for N<sub>2</sub>O and N<sub>2</sub> concentration analysis by an auto-sampler robotized incubation system (ROBOT), as described by Molstad et al. [34]. Triplicate vials were destructively sampled on days 0, 1, and 14 for molecular analysis.

The auto-sampler ROBOT system, equipped with a gas chromatograph (GC) (7890 A, Agilent, USA), was used to measure the kinetics of gaseous N. Briefly, a peristaltic pump transferred the headspace gas from the incubation vials to the GC system, where N<sub>2</sub>O and N<sub>2</sub> concentrations were determined using an electron capture detector and a thermal conductivity detector, respectively. Besides measuring the N<sub>2</sub>O and N<sub>2</sub> accumulation during the anoxic incubation, the N<sub>2</sub>O index ( $I_{N_2O}$ ) was also calculated to characterize the N<sub>2</sub>O production ratio expressed as N<sub>2</sub>O/(N<sub>2</sub>O+N<sub>2</sub>) as described previously [12].  $I_{N_2O}$  formula is:

$$I_{N_2O} = \int_0^{t_{end}} N_2O(t) dt / \int_0^{t_{end}} [N_2O(t) + N_2(t)] dt$$

where  $N_2O(t)$  represents the accumulation of  $N_2O$  at any time  $t$ ,  $N_2(t)$  represents the accumulation of  $N_2$  at any time  $t$ , and  $t_{end}$  is the end time of the incubation.

#### Soil DNA extraction and bioinformatics used for the community analysis

DNA was extracted from 0.3 g of frozen soil samples for each replicate using the FastDNA SPIN Kit (MP Bio-medicals, USA), following the manufacturer's instructions. A total of 54 DNA samples were collected from six treatment groups (triplicates per group) at three different time points (day 0, day 1, and day 14). The universal primers 341F and 785R were used to amplify the V3-V4 region of the 16S rRNA gene amplicons according to the Illumina MiSeq platform protocol (Illumina Inc., USA). PCR amplification was performed in triplicate for each DNA sample, and the purified amplified products were sequenced using an Illumina MiSeq system as described previously [9, 35].

The 16S rRNA gene sequence data was imported and pre-processed in QIIME [36] to check the quality and quantity of sequences and remove adapter sequences. The adapter-trimmed sequences were denoised, and the forward and reverse sequence reads were spliced together using DADA2 [37]. Specifically, the forward and reverse reads were truncated at positions 275 and 175, respectively, while discarding reads shorter than these values. A minimum 20-nucleotide overlap between the forward and reverse reads was required. Untrusted or chimeric sequences were eliminated, and taxonomy was assigned using the SILVA 138 database. A phylogenetic tree was constructed using FastTree [38]. The amplicon sequence variants (ASV) table was rarefied to a depth of 11,000 sequences per sample with 5,000 permutations before computing diversity metrics.

#### Quantitation of nitrogen cycling genes

The quantity of extracted DNA was measured using the PicoGreen dsDNA Assay Kit (Quanti-iT PicoGreen, Invitrogen, USA) on a multi-mode microplate reader (SpectraMax iD5, USA) and used as the template. The copy numbers of bacterial denitrification-related genes were determined by quantitative PCR (qPCR) using a fluorescence quantitative PCR instrument (qTOWER3G touch, Analytik Jena, Germany). The primers and PCR conditions used for amplification were as described previously [9, 10]. Specifically, the bacterial *narG*, *nirS*, *nirK*, and *nosZ* genes were amplified using the primers narG-f/narG-r, nirS-cd3aF/nirS-R3cd, nirK-1040/F1aCu, and nosZ-2f/2r, respectively (Table S2).

#### Metagenome sequencing and data analysis

To investigate the microbiome's ecological functions across different treatment groups, soil samples from day 0 and day 14 were selected for metagenomic sequencing. The whole-genome shotgun (WGS) approach was employed to sequence total metagenomic DNA from the soil samples using the Illumina Novaseq high-throughput sequencing platform (Shanghai Majorbio Bio-pharm Technology Co., Ltd.). The sequencing was conducted with  $2 \times 150$  bp paired-end reads, following the construction of a sequencing library from fragmented soil DNA.

Unless specified otherwise, all software used in this study utilized default parameters. Quality control of the raw sequencing data was performed using Fastp (v0.20.0) [39], resulting in a clean dataset for subsequent analysis. Contigs  $\geq 300$  bp were retained after the clean reads were assembled into contigs using MEGAHIT (v1.1.2) [40]. Coding sequences within the contigs were predicted using Prodigal (v2.6.3) [41]. The contigs were then clustered with 95% similarity and 90% alignment coverage to generate a non-redundant contig set using linclust mode of MMseqs2 [42]. Species annotation of the non-redundant gene sets was conducted by aligning them to the NCBI non-redundant (NR) database using BLASTP (v2.2.28+) with the DIAMOND (v2.0.13) [43] software program, employing the best-hit species annotation method. For functional gene annotation, the non-redundant gene set sequences were aligned to the Kyoto Encyclopedia of Genes and Genomes (KEGG) database using DIAMOND [43], and the predicted genes were annotated using KOBAS (v2.0) [44]. Gene abundance profiles were calculated using transcripts per million (TPM), which corresponds to mapped reads in this study. The TPM values were used to normalize the effects of total read counts and gene lengths, facilitating the comparison of gene abundances between samples [45].

#### Statistical analysis

The fold change of ASV abundance differences between soils and extracted cells for the initial 16S rRNA gene V3-V4 region sequences was generated using the edgeR package [46] with an exact test. Taxonomy was assigned to ASVs only if their abundance differed by more than fivefold with a  $p < 1 \times 10^{-5}$  in the exact test output.

The statistical significance of the gas kinetics, the quantity of denitrifying genes, and the relative abundance of denitrifying genes based on metagenomic data was determined by a two-way analysis of variance (ANOVA) with a post hoc Tukey's multiple comparisons test. Furthermore, significant differences in overall bacterial alpha diversity, denitrifying bacterial community alpha diversity indices, and the relative abundance of denitrifying bacterial genera between FS and BS across different treatment groups were determined using the Kruskal-Wallis

statistical test. Additionally, Principal Coordinates Analysis (PCoA) based on Bray-Curtis distance was performed to construct ordination plots and visualize shifts in overall bacterial community composition and denitrifying bacterial communities across different treatments. These dissimilarity patterns were confirmed by the Analysis of Similarities (ANOSIM) test using the vegan package [47].

Furthermore, biomarker denitrifying species were identified using Linear Discriminant Analysis Effect Size (LEfSe) with parameters of  $p < 0.05$  and LDA score  $> 2$  [48]. Spearman's correlation between LEfSe-derived key denitrifying species and  $N_2O$  accumulation was performed in MATLAB 2022a.

The relationship between soil type, denitrifying communities, and the  $N_2O$  index was explored using partial least squares path modeling (PLSPM). In the PLSPM model, the estimates of the coefficients of determination ( $R^2$ ) and the path coefficient (direct effect) were validated using the plspm package [49] with 1000 bootstraps.

Finally, all data were graphed using GraphPad Prism version 8.0 and R version 4.3.1 [50].

## Results

### Physicochemical properties of the two soils

The physicochemical properties of FS and BS displayed significant differences, as detailed in Table 1. Specifically, BS exhibited markedly higher values for moisture content, WHC,  $NO_3^-$ , and dissolved organic carbon (DOC) content compared to FS. Conversely, BS demonstrated a significantly lower  $NH_4^+$  content. Additionally, the pH values differed substantially between the two samples: BS presented an acidic pH of 6.5, whereas FS showed an alkaline pH of 8.2.

### Microbial cell extraction bias

To evaluate the representativeness of extracted cells to soil bacteriomes, 16S rRNA gene amplicon sequencing was employed. The ASVs predominantly correlated with their soil origin, as evidenced by the clustering of extracted cells near their original soils on the PCoA plot, distinct from other soils (ANOSIM:  $R=0.97$ ,  $p=0.002$ ,

Fig. S2a). This analysis also revealed inter-soil differences. Non-significant changes were detected between extracted cells and their origin soils, both shared a substantial proportion of ASVs (mean 56.5%, standard deviation 10.8%) (Fig. S2b). Further, ASV detection bias was evident at the phylum level (Fig. S2c), with Acidobacteria being more prevalent in soils and Firmicutes in extracts. Differential abundance analysis using an exact test identified specific organisms with varying relative extractability (Fig. S2d). ASVs linked to Pyrinomonadaceae (Acidobacteria) and Bacillaceae (Firmicutes) were significantly less and more abundant in extracted cells compared to soils, respectively, with no other consistent extraction biases observed.

To further investigate the functional relatedness of extracted cells in comparison to soil bacteriomes, we analyzed the differences in  $N_2O$  accumulation dynamics between original soils and their corresponding cell extracts. For FS (Fig. S3a), the cell extract accumulated relatively less  $N_2O$  compared to the soil, although the overall trend of gas peaking and declining remained consistent between the two. In contrast, for BS (Fig. S3b), the cell extract exhibited a similar  $N_2O$  accumulation to that of the soil, with a slightly quicker onset of accumulation. These findings demonstrate a functional similarity, indicating that the  $N_2O$  accumulation profiles between cell extracts and their corresponding soils did not differ significantly.

### Comparison of gas kinetics during anoxic incubation

For the  $N_2O$  kinetics, in the NSC group (Fig. 1a),  $N_2O$  accumulation was significantly higher in the BS compared to FS throughout the incubation. Peak  $N_2O$  concentrations in BS reached approximately  $8 \times 10^3$  nmol  $g^{-1}$  dry soil around 74 h, while FS maintained lower levels, peaking at around  $4 \times 10^3$  nmol  $g^{-1}$  dry soil and completely depleted until 150 h while continued to decrease gradually in BS. The FSB treatment (Fig. 1b) showed a dramatic increase in  $N_2O$  accumulation in BS from 242 h onwards, reaching nearly  $9 \times 10^3$  nmol  $g^{-1}$  dry soil by 314 h. In contrast, FS exhibited lower  $N_2O$  levels that completely declined before 74 h. The BSB group (Fig. 1c) on the other hand, demonstrated that BS had a notable increase in  $N_2O$  levels, peaking above  $9 \times 10^3$  nmol  $g^{-1}$  dry soil around 38 h and gradually started declining afterwards. Whereas, FS treatment in the BSB group also showed an increase but peaked earlier at around  $7 \times 10^3$  nmol  $g^{-1}$  dry soil by 26 h, followed by a sharp decline.

In the NSC group (Fig. 1d), accumulation area under the dynamic curve of  $N_2O$  was significantly ( $p < 0.001$ ) greater in BS compared to FS at all time points after 50 h. The FSB group (Fig. 1e) also exhibited significantly ( $p < 0.001$ ) higher  $N_2O$  accumulation in BS than FS, especially notable after 98 h. The total  $N_2O$  accumulation

**Table 1** Differences in physicochemical properties of the two soils, displayed as mean values with SD from triplicate samples per treatment

	FS	BS	Sig
Moisture content %	2.3 ± 0.04	14.8 ± 0.08	***
WHC %	45.1 ± 0.47	48.7 ± 0.40	**
pH	8.2 ± 0.02	6.5 ± 0.01	***
$NO_3^-$ (mg/Kg soil)	1.2 ± 0.17	10.9 ± 3.41	**
$NO_2^-$ (mg/Kg soil)	0	0	–
$NH_4^+$ (mg/Kg soil)	10.9 ± 0.39	7.5 ± 0.93	**
DOC (mg/kg)	18.08 ± 0.96	26.95 ± 1.11	**

Sig=Significance. \*\*  $p \leq 0.01$ ; \*\*\*  $p \leq 0.001$

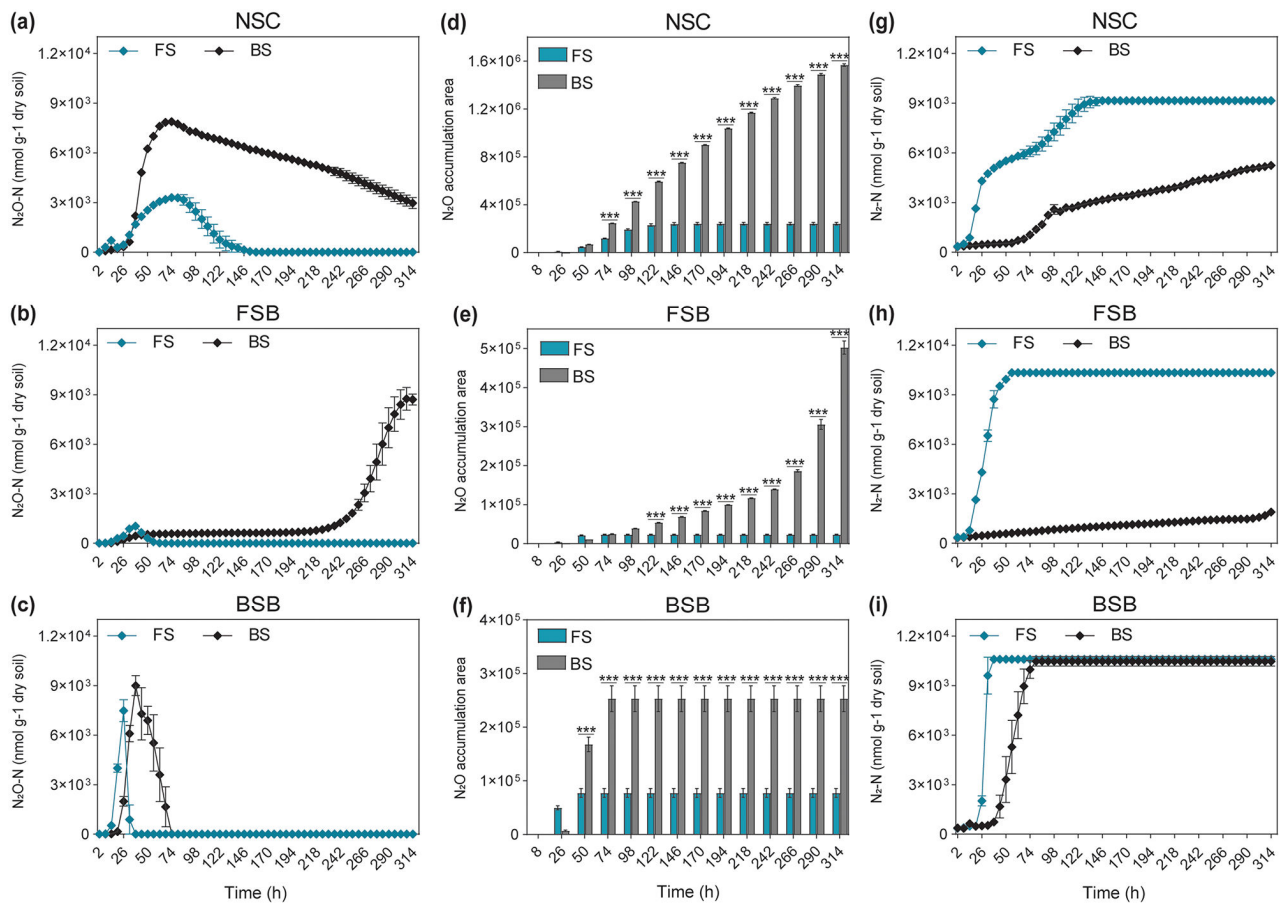


**Fig. 1** Dynamics of gas kinetics during anoxic incubation. Comparison of  $N_2O$  (a–c) and  $N_2$  (g–i) kinetics, and  $N_2O$  accumulation area (d–f) between FS and BS across three different treatment groups: NSC, FSB, and BSB. Bars indicate means, and error bars represent the standard error of the mean (SEM). Significant differences are calculated via two-way ANOVA followed by Tukey’s multiple comparisons test and are indicated by asterisks (\*  $p < 0.05$ , \*\*  $p < 0.01$ , \*\*\*  $p < 0.001$ )

area of BS was 6.50 and 21.74 times higher than that of FS in both groups respectively. In the BSB group (Fig. 1f), accumulation area under the dynamic curve of  $N_2O$  was consistently higher in BS compared to FS, with significant differences ( $p < 0.001$ ) observed from 50 h onwards and the total accumulation area of BS was 3.26 times greater than that of FS.

The  $N_2$  accumulation by FS was much higher than BS in all groups. In the NSC group (Fig. 1g),  $N_2$  accumulation was consistently higher in FS compared to BS throughout the incubation, peaking above  $9 \times 10^3$  nmol  $g^{-1}$  dry soil. For the FSB group (Fig. 1h), FS exhibited a rapid increase in  $N_2$  levels, stabilizing above  $9 \times 10^3$  nmol  $g^{-1}$  dry soil before 50 h, while BS showed a super delayed and minimal accumulation. In the BSB group (Fig. 1i), compared to BS, which peaked by 74 h, FS showed a rapid increase in  $N_2$  levels, peaking above  $9 \times 10^3$  nmol  $g^{-1}$  dry soil by 26 h which is quite early in the incubation.

The difference in the accumulation area under the dynamic curve of  $N_2$  in FS and BS was significant ( $p < 0.001$ ) throughout the incubation in all groups. The

total  $N_2$  accumulation area in FS was 1.11–9.16 times greater than that in BS depending on the group (Fig. S4a–c).

Furthermore, in NSC and FSB groups (Fig. S4d–e), area under the dynamic curve of  $N_2O + N_2$  increased over time for both FS and BS. The FS consistently exhibited higher accumulation compared to BS, with significant ( $p < 0.001$ ) differences observed throughout from 50 h. For the BSB group (Fig. S4f), though  $N_2O + N_2$  accumulation was higher for FS but the differences were nonsignificant. The total accumulation area of  $N_2O + N_2$  for FS was 1.06, 3.6, and 1.04 times greater than that of BS in NSC, FSB, and BSB, respectively.

The  $N_2O/(N_2O + N_2)$  ratio was significantly ( $p < 0.001$ ) higher in BS than in FS across all groups (Table 2). These results highlight significant differences in  $N_2O$  and  $N_2$  accumulation dynamics between FS and BS across the different treatments. The two-way ANOVA results (Table S3) further confirm the significant effects of both soil types (FS and BS) and treatments (whether inoculation with FS- or BS-derived bacteriomes [FSB, BSB] or leaving

**Table 2** N<sub>2</sub>O ratios calculated as N<sub>2</sub>O/N<sub>2</sub>O + N<sub>2</sub> based on the area under the curve (AUC) for N<sub>2</sub>O relative to the total gas production (N<sub>2</sub>O + N<sub>2</sub>) over the entire incubation period and displayed as mean values with SEM from triplicate vials per treatment

	FS	BS	Sig
NSC	0.092 ± 0.011	0.631 ± 0.014	***
FSB	0.007 ± 0.001	0.608 ± 0.012	***
BSB	0.025 ± 0.001	0.08 ± 0.004	**

Sig=Significance. \*\*  $p \leq 0.003$ ; \*\*\*  $p \leq 0.001$

the soils untreated [NSC]), with notable interactions influencing N<sub>2</sub>O accumulation across the treatments.

### Comparison of denitrification functional genes

Based on metagenomic sequence analysis, we evaluated the variations in relative abundances of various denitrification genes between FS and BS in initial soils and samples after 14 days of anoxic incubation. In the NSC group (Fig. 2a-b), the relative abundances of *narG* and *nirK* were significantly higher ( $p < 0.001$ ) in FS compared to BS, both initially and after 14 days of incubation. While the initial relative abundances of *napA*, *nirS*, and *nosZ* were also higher in FS, their differences became statistically significant ( $p < 0.001$ ) after 14 days. Initially, *norB* and *norC* exhibited slightly higher relative abundances in BS; however, this trend reversed after 14 days, though the differences were not statistically significant.

The initial relative abundances of the genes *narG*, *nirK*, *nirS*, and *nosZ* between the FSB and BSB bacteriomes (Fig. 2c) were observed to be higher in the FSB group compared to the BSB group, with the differences in *narG* and *nirK* abundances being statistically significant ( $p < 0.001$ ). After 14 days, within the FSB group (Fig. 2d), the relative abundance of *nirK* was significantly elevated in the BS compared to the FS ( $p < 0.001$ ). Conversely, the relative abundances of *napA*, *napB*, *nirS*, *norB*, *norC*, and *nosZ* were higher in the FS, with the latter three genes showing statistically significant differences ( $p < 0.01$ ). In the BSB group (Fig. 2e), the abundance of *nirK* was also significantly higher in the BS compared to the FS ( $p < 0.001$ ). Although *norB*, *norC*, and *nosZ* exhibited higher abundances in the BS, these differences were not statistically significant. In contrast, the relative abundances of *narG* and *narH* were significantly higher in the FS compared to the BS ( $p < 0.001$ ).

In addition, the ratios of *nirK/nosZ* (Fig. 2f) were higher in BS compared to FS across all groups with significant difference ( $p < 0.001$ ) in FSB group. Whereas, the ratios of *nirS/nosZ* (Fig. 2g) were higher in FS compared to BS, with significant differences ( $p < 0.01$ ) in the NSC and BSB groups.

The quantified abundances of the four denitrifying functional genes, *narG*, *nirK*, *nirS*, and *nosZ*, determined

by qPCR, exhibited trends consistent with the metagenomic sequencing data. After 14 days (Fig. S5a-d), in the NSC group, the copy numbers of all four genes were significantly higher in the FS compared to the BS. In the FSB and BSB groups, the copy numbers of the *nirS* gene were higher in the FS, while the *nirK* gene copies were more abundant in the BS. Notably, the ratios of *nirK* and *nirS* to *nosZ* (Fig. S5e-f) revealed higher *nirK/nosZ* ratios in the BS and higher *nirS/nosZ* ratios in the FS across all groups, paralleling the trends observed in the metagenomic data.

We observed significant main and interaction effects of soil types and treatments on the abundance of denitrification genes (Table S4), highlighting their influence on denitrification dynamics.

### Bacterial community composition and diversity

The PCoA plots (Fig. 3a) based on the Bray-Curtis distance of the 16S rRNA gene V3-V4 region sequences, illustrate the variations in microbial community composition among the groups. The ANOSIM results indicate statistically significant ( $p = 0.001$ ) differences in the microbial community composition between FS and BS across the groups ( $R = 0.99, 0.92, \text{ and } 0.77$ , for NSC, FSB, and BSB, respectively). The ANOSIM values reveal significant temporal shifts within microbial communities, particularly in the inoculated groups (FSB and BSB). The same initial inoculum diverged markedly between FS and BS after 14 days of incubation, highlighting a strong impact of recipient soil on microbial community structure.

The alpha diversity metrics, based on 16S rRNA gene V3-V4 region sequences, including the observed features (Fig. 3b) and Shannon index (Fig. 3c), reveal significant differences between FS and BS across the groups (NSC, FSB, BSB) over time. In the FSB and BSB groups, these features showed a significant decrease ( $p < 0.001$ ) towards the end of incubation. Conversely, the NSC group exhibited significant ( $p < 0.001$ ) increase and decrease in diversity for FS and BS, respectively. These results underscore the differential impacts of the recipient soil environment on microbial diversity and richness over time.

The number of clean metagenome sequence reads in the samples varied from 101,115,944 to 126,434,714. The relative abundance of reads with no BLAST hit ranged from 62.4 to 78.8%, depending on the sampling time (higher in samples at the initial time point) and treatment type. The relative abundance of bacterial phyla varied significantly across treatment groups over time (Fig. S6). Initially, Pseudomonadota, Actinomycetota, and Acidobacteriota were predominant in all groups. By the end of the incubation, the bacterial community composition in the NSC group remained relatively stable. In contrast, the FSB and BSB groups exhibited substantial shifts.

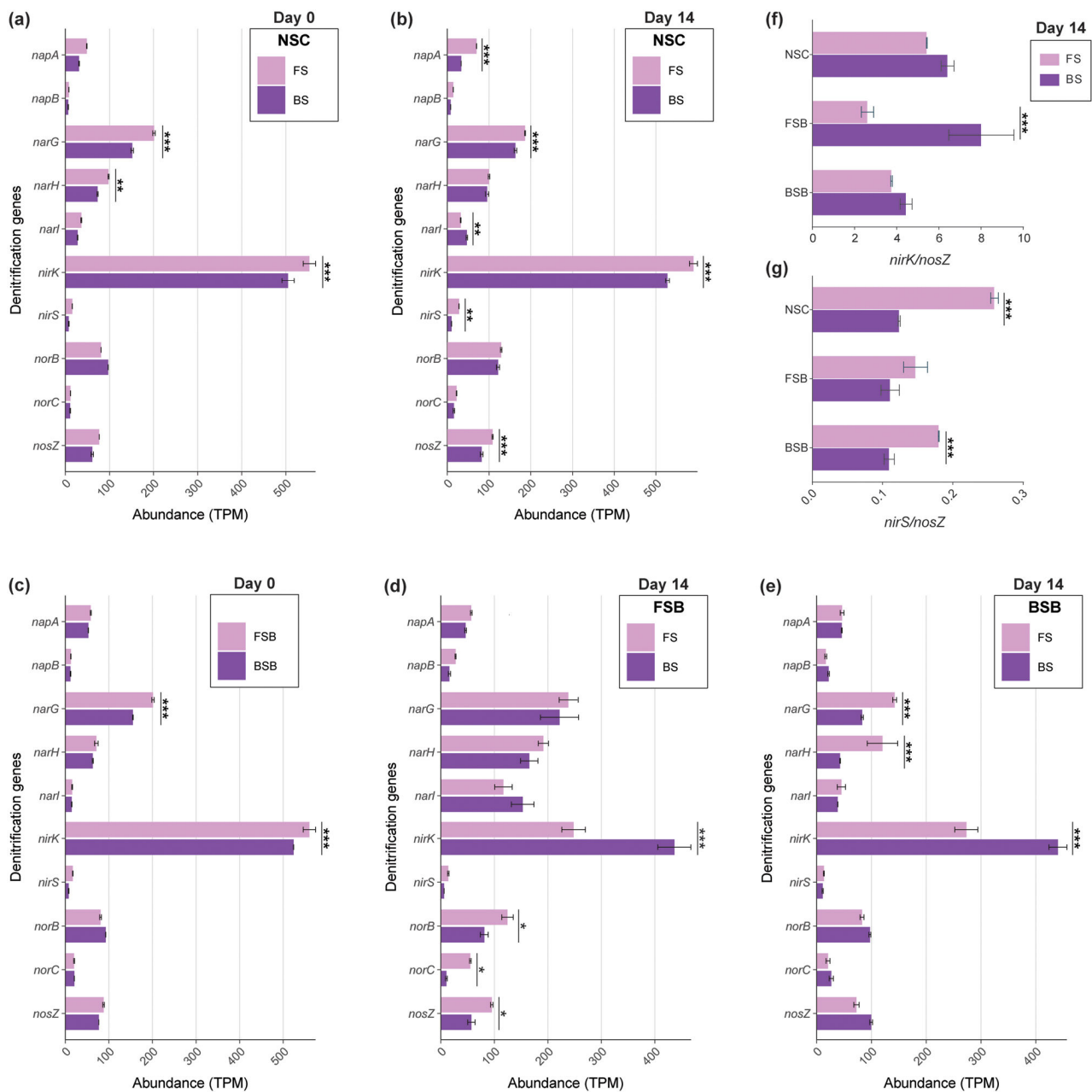


**Fig. 2** Comparison of shifts in relative abundances of denitrification genes between FS and BS across different treatment groups (NSC, FSB, and BSB) during anoxic incubation from Day 0 to Day 14. **(a)** Gene relative abundances in the NSC group at Day 0. **(b)** Gene relative abundances in the NSC group at Day 14. **(c)** Gene relative abundances of FSB and BSB bacteriome at Day 0. **(d)** Gene relative abundances of FS and BS in the FSB group at Day 14. **(e)** Gene relative abundances of FS and BS in the BSB group at Day 14. **(f)** Differences in the ratios of *nirK/nosZ* between FS and BS across the treatment groups. **(g)** Differences in the ratios of *nirS/nosZ* between FS and BS across the treatment groups. Gene abundance is expressed in TPM, with data derived from metagenome sequencing. Significant differences between FS and BS are calculated via two-way ANOVA and denoted by asterisks (\*  $p < 0.05$ , \*\*  $p < 0.01$ , \*\*\*  $p < 0.001$ )

Both groups demonstrated a marked decline in the relative abundance of Actinomycetota and Acidobacteriota. In the FSB group, there was a significant increase in the abundance of Pseudomonadota and Bacillota in both FS and BS. Meanwhile, the BSB group showed a substantial increase in Bacteroidota in both FS and BS, and a notable increase in Gemmatimonadota in the BS.

Based on metagenome sequencing data, initially, a substantial proportion of bacterial taxa remained unclassified at the genus level across all treatment groups (NSC, FSB, BSB), with percentages ranging from 65.0 to 78.3% (Fig. 3d). By the end of the incubation period, the proportion of unclassified bacterial communities remained relatively stable in the NSC group (67.6–68.5%). However,

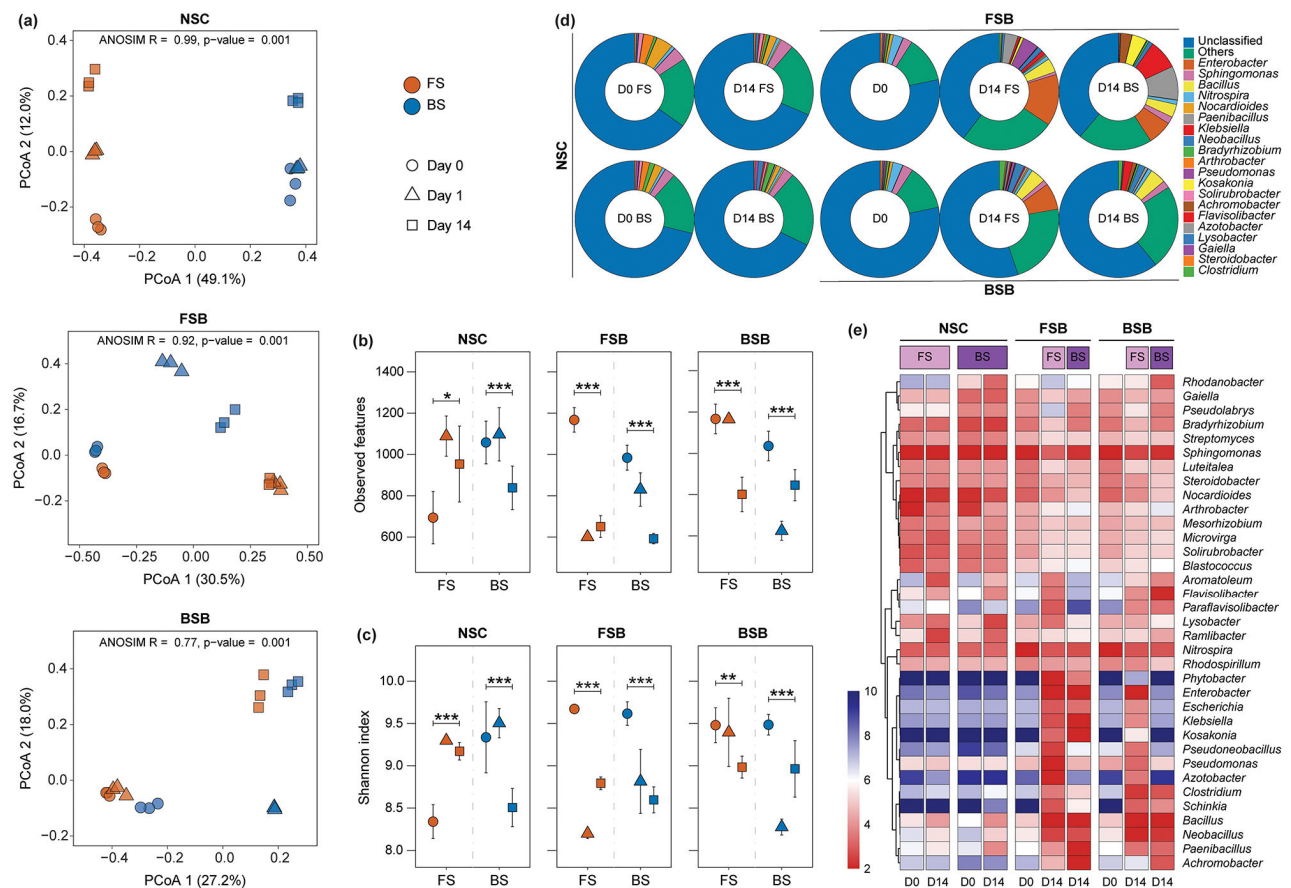


**Fig. 3** Comparison of microbial community composition and diversity between FS and BS across different treatment groups (NSC, FSB, and BSB) during anoxic incubation over time. **(a)** PCoA plots of microbial communities based on Bray-Curtis dissimilarity in NSC, FSB, and BSB treatment groups. ANOSIM R and  $p$ -values indicate the strength and significance of differences between FS and BS. **(b)** Observed features and **(c)** Shannon diversity index in NSC, FSB, and BSB groups at different time points, based on 16 S rRNA gene sequencing data. Significant differences between FS and BS are calculated via the Kruskal-Wallis test and denoted by asterisks (\*  $p < 0.05$ , \*\*  $p < 0.01$ , \*\*\*  $p < 0.001$ ). **(d)** Relative abundance of dominant bacterial taxa at the genus level in NSC, FSB, and BSB groups over time for FS and BS. **(e)** Heatmap showing variations in the relative abundance of dominant bacterial genera in NSC, FSB, and BSB groups over time for FS and BS, based on metagenome sequencing data. Color intensity represents the log-transformed relative abundance of each genus

there was a notable reduction in the FSB (38.8 – 39.7%) and BSB (55.1 – 60.8%) groups. Although several genera such as *Spingomonas*, *Nitrospira*, *Bradyrhizobium*, and *Nocardioideles* remained relatively consistent across the groups over time, significant shifts in microbial community structure were evident (Fig. 3e). In the NSC group, genera such as *Flavisolibacter*, *Aromatoleum*, *Lysobacter*, and *Ramlibacter* showed enrichment in both FS and BS over time. The FSB group displayed a significant increase in the relative abundance of *Flavisolibacter*, *Aromatoleum*, *Lysobacter*, *Pseudomonas*, and *Azotobacter* in FS, while *Pseudolabrys* and *Bradyrhizobium* were enriched in BS. In the BSB group, there was a marked increase in the abundance of *Flavisolibacter*, *Aromatoleum*, *Clostridium*, *Bacillus*, *Neobacillus*, and *Paenibacillus* in both FS and BS. Additionally, *Pseudomonas*, *Azotobacter*, *Enterobacter*, *Klebsiella*, and *Kosakonia* were particularly enriched in FS, whereas *Achromobacter* was notably enriched in

BS. These observations indicate a shift in taxon composition under different soil conditions.

### Comparison of denitrifying community composition

Based on the analysis of metagenome sequence data, the taxonomic composition of dominant denitrifying genera exhibited significant shifts across different treatment groups over time (Fig. 4). In the NSC group, *Ramlibacter*, which contains the *narG* (Fig. 4a), *nirK* (Fig. 4b), *nirS* (Fig. 4c), *norB* (Fig. 4d), and *nosZ* (Fig. 4e) genes, was enriched in both FS and BS, with a notably higher enrichment in FS. This suggests a greater overall denitrification potential in FS. In the FSB group, potential complete denitrifiers such as *Pseudomonas*, which contains *narG*, *nirS*, *norB*, and *nosZ*, and *Stutzerimonas*, which contains *nirS*, *norB*, and *nosZ*, were significantly enriched only in FS. In contrast, *Paenibacillus*, *Achromobacter*, and *Geobacillus*, which contain only *nirK*, were highly enriched in

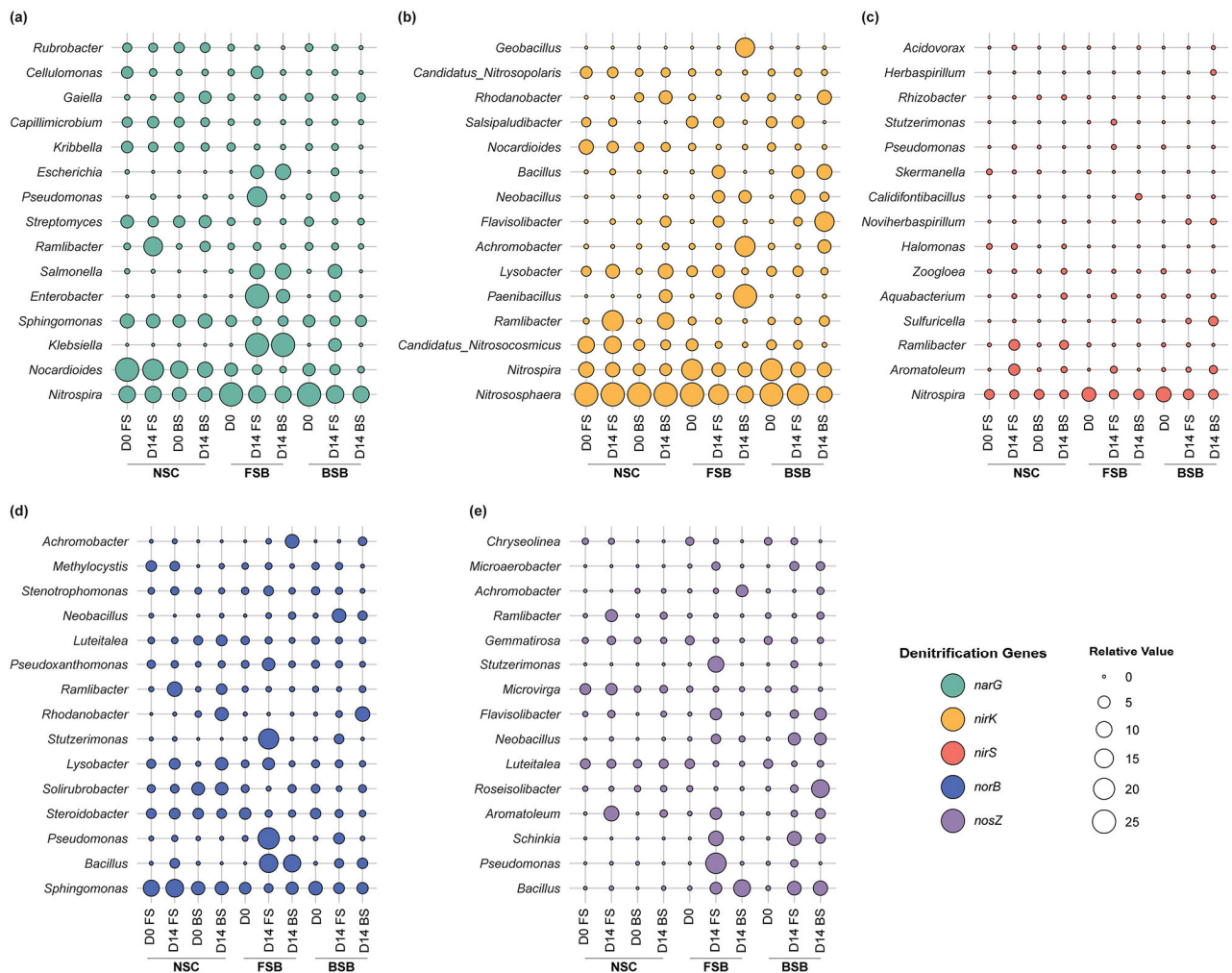


**Fig. 4** Shifts in the relative abundance of dominant denitrifying bacterial genera between FS and BS across different treatment groups (NSC, FSB, and BSB) over time during anoxic incubation. **(a)** Relative abundance of dominant *narG* gene-containing bacterial genera. **(b)** Relative abundance of dominant *nirK* gene-containing bacterial genera. **(c)** Relative abundance of dominant *nirS* gene-containing bacterial genera. **(d)** Relative abundance of dominant *norB* gene-containing bacterial genera. **(e)** Relative abundance of dominant *nosZ* gene-containing bacterial genera. The size of the circles represents the relative abundance of each denitrifying taxon, while different colors correspond to different denitrification genes, all based on metagenome sequencing data

BS. Similarly, in the BSB group, *Neobacillus*, which contains *nirK*, *norB*, and *nosZ*, was predominantly enriched in FS, while *nirK*-containing *Flavisolibacter* and *nosZ*-containing *Roseisolibacter* were highly enriched in BS. In addition, genus *Rhodanobacter*, containing *nirK* and *norB*, was highly enriched only in the BS of both NSC and BSB groups but declined in the FS of BSB, despite having the same initial inoculum. Overall, these taxonomic variations indicate clear shifts in denitrifying genera based on the recipient soil environment.

Further statistical analysis revealed significant differences in the relative abundance of denitrifying genera between FS and BS across all treatment groups (Fig. 5 and Fig. S7). For the *nirK*-based genera, the relative abundance of *Nitrososphaera* and *Aromatoleum* was significantly higher in FS ( $p < 0.001$ ), whereas *Rhodanobacter*, *Flavisolibacter*, and *Bradyrhizobium* were more

abundant in BS (Fig. S7a-c). In contrast, for *nirS*-containing genera, *Aromatoleum* and *Pseudomonas* were significantly more abundant in FS ( $p < 0.001$ ). However, no *nirS*-containing genus showed a consistent enrichment in BS across the groups (Fig. S7d-f). Furthermore, similar to the *nirS*-based denitrifiers, *Aromatoleum* and *Pseudomonas*, along with some other genera, appeared as *norB* and *nosZ*-based denitrifying genera with a significantly higher relative abundance in FS ( $p < 0.001$ ). Conversely, *Solirubrobacter* was identified as a *norB*-based denitrifier, and *Rhodanobacter* emerged as both *norB*- and *nosZ*-based denitrifier, predominantly in BS across the groups (Fig. 5a-f). In addition, based on PICRUSt2 predictions from the 16S rRNA gene V3-V4 region sequences, the number of taxa predicted to be harbouring a complete denitrification pathway was higher in FS compared to BS across all treatment groups (Table S5).

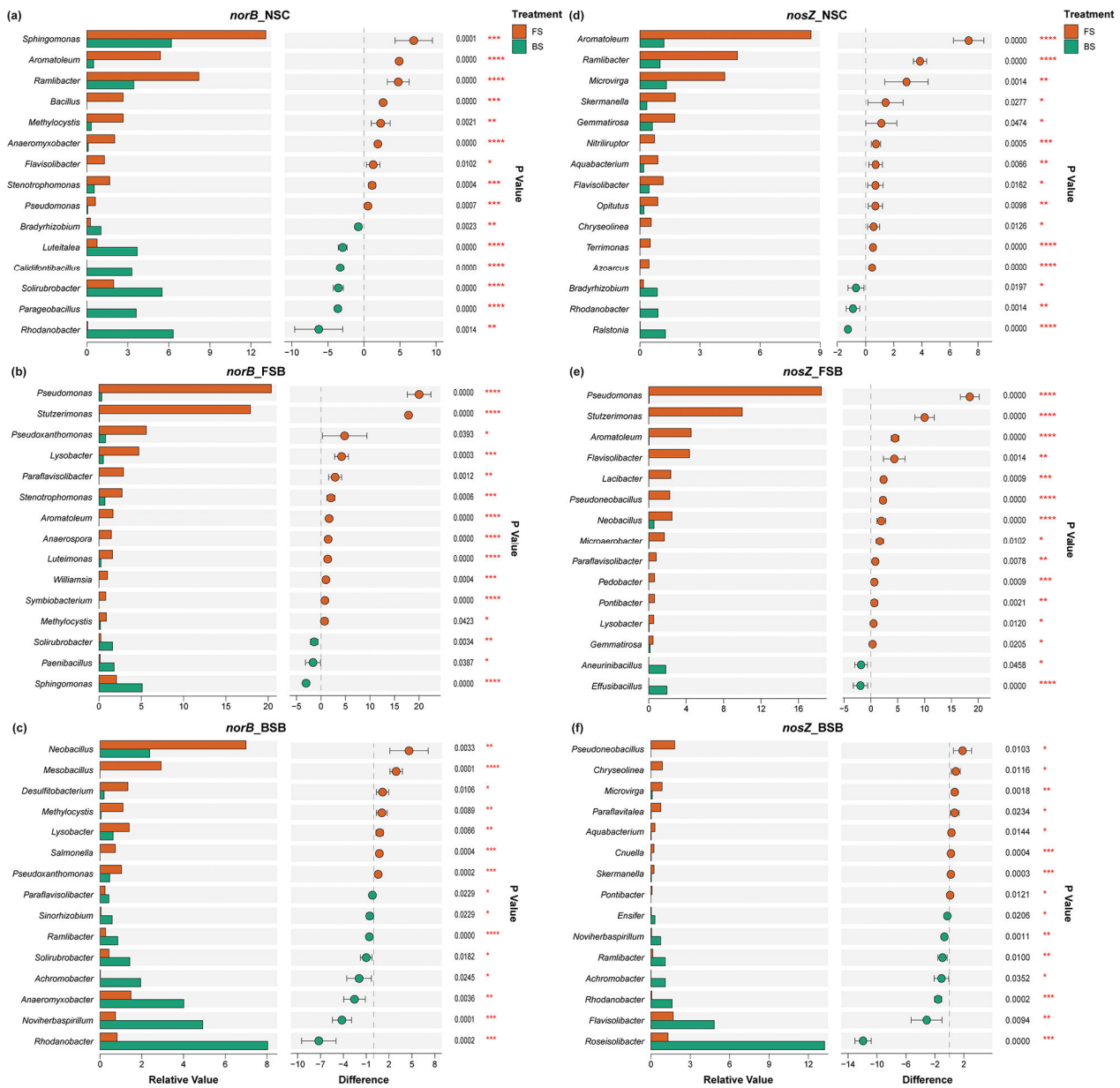


**Fig. 5** Differences in the relative abundance of denitrifying genera containing *norB* and *nosZ* genes between FS and BS across different treatment groups at the end of anoxic incubation. Relative abundance of bacterial genera in FS and BS containing the *norB* gene in (a) NSC, (b) FSB, and (c) BSB groups. Relative abundance of bacterial genera in FS and BS containing the *nosZ* gene in (d) NSC, (e) FSB, and (f) BSB groups. The left panels display bar plots of the relative abundance of each genus, while the dot plots in the right panels show the confidence intervals (CI) for the differences in relative abundance between FS and BS. Significant differences are calculated via the Kruskal-Wallis test and denoted by asterisks (\*  $p < 0.05$ , \*\*  $p < 0.01$ , \*\*\*  $p < 0.001$ , \*\*\*\*  $p < 0.0001$ ). Data to calculate the differences in the relative abundance of denitrifying genera is based on metagenome sequencing

The alpha diversity and PCoA of the Bray-Curtis distance, based on metagenomic sequencing results, reveal significant differences in the microbial communities involved in denitrification between FS and BS across the treatment groups. The Shannon index (Fig. 6a and b, and Fig. S8a and b) and observed features (Fig. 6c and d, and Fig. S8c and d) for the *nirK*-, *nirS*-, *norB*-, and *nosZ*-containing bacterial communities significantly ( $p < 0.001$ )

increased towards the end of incubation in both FS and BS of the NSC and BSB groups, with a more pronounced increase in FS. In contrast, the FSB group showed a divergent pattern: the Shannon index for *nirK* (Fig. S8a) and *nirS* (Fig. S8b) based communities increased significantly ( $p < 0.001$ ) in FS but decreased in BS. Furthermore, for the *norB* and *nosZ* communities, the Shannon index decreased in both FS and BS compared to the

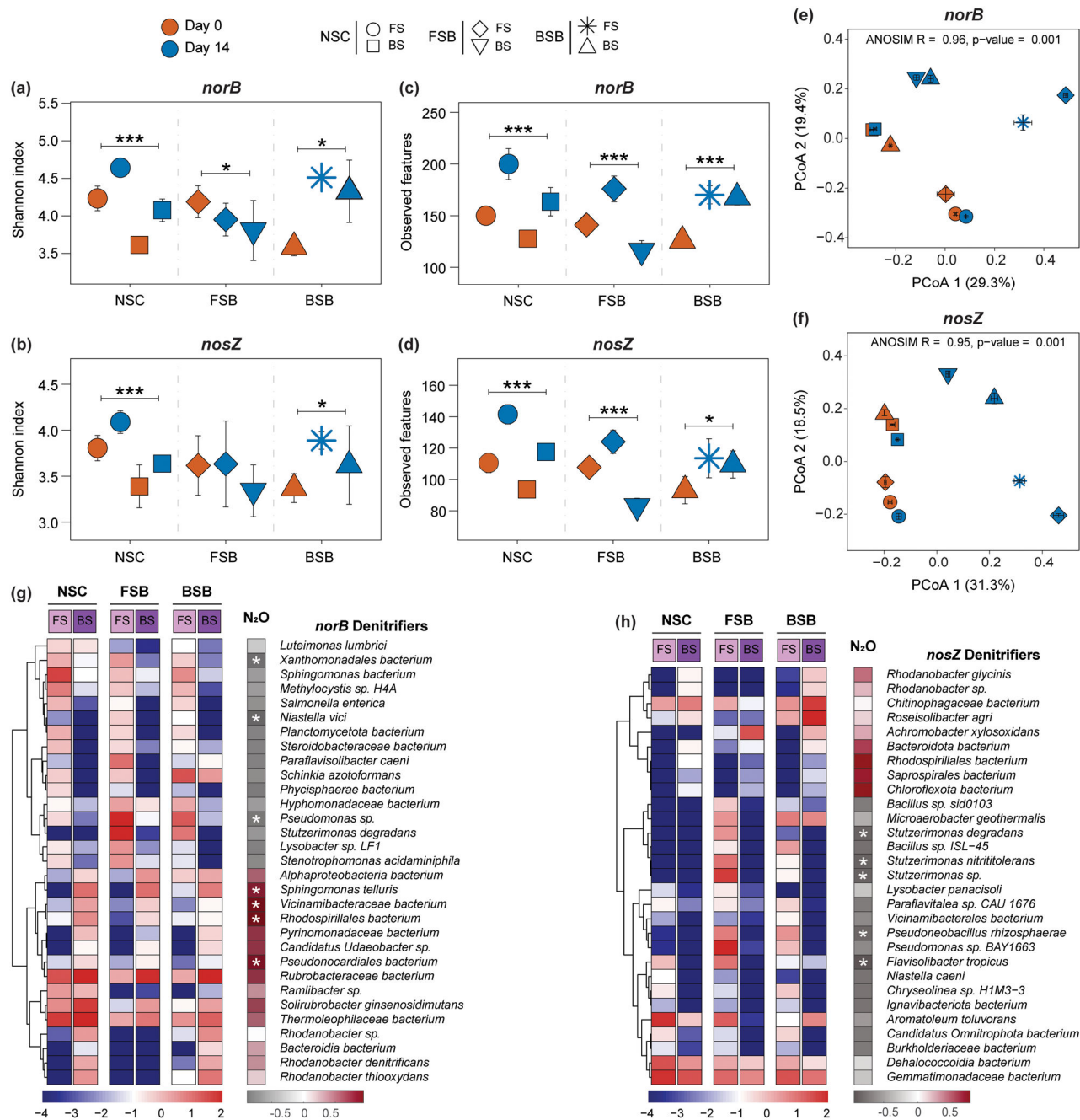


**Fig. 6** Diversity and composition of key denitrifiers between FS and BS across different treatment groups (NSC, FSB, and BSB) during anoxic incubation over time. Shannon index of the (a) *norB* and (b) *nosZ* denitrifying community and observed features of the (c) *norB* and (d) *nosZ* denitrifying community at Day 0 and Day 14 between FS and BS across NSC, FSB, and BSB treatment groups. Significant differences are calculated by the Kruskal-Wallis test and denoted by asterisks (\*  $p < 0.05$ , \*\*\*  $p < 0.001$ ). PCoA plots of microbial communities based on the (e) *norB* and (f) *nosZ* denitrifying community structure at Day 0 and Day 14 across NSC, FSB, and BSB treatment groups. ANOSIM R and p-values indicating significant separation. Heatmaps of LefSe-derived key (g) *norB* denitrifiers and (h) *nosZ* denitrifiers, discriminating between FS and BS across NSC, FSB, and BSB groups at Day 14. The colors scheme in the left panel represent the log-transformed relative abundance of the key species in each sample, while those in the right panel denote the R-value of Spearman's correlation between key species and N<sub>2</sub>O accumulation (\* indicates  $p < 0.05$ ). Data used for Fig. 6 is based on metagenome sequencing

initial time point. Similarly, the observed features for the FSB group increased significantly ( $p < 0.001$ ) in FS but decreased in BS over time for the *nirS* (Fig. S8d), *norB* (Fig. 6c), and *nosZ* (Fig. 6d) based communities, whereas

for the *nirK*-based community (Fig. S8c), a decrease was observed in both FS and BS compared to the initial community. Additionally, the PCoA plots (Fig. 6e and f, and Fig. S8e and f) demonstrated significant differences

( $p=0.001$ , ANOSIM test) and clear clustering of denitrifying bacterial communities across the NSC, FSB, and BSB treatment groups between FS and BS over time. These findings elucidate the differential impacts of the recipient soil conditions on the composition and diversity of the denitrifying microbial communities as evolved over time.

#### Correlation between the abundance of key denitrifiers and N<sub>2</sub>O accumulation

The output files of the species level abundance data from the metagenome sequencing were used as input for the LEfSe algorithm to identify key *nirK*, *nirS*, *norB*, and *nosZ*-related species in FS and BS across different treatment groups. Subsequently, key species with significant differences in relative abundance between FS and BS were further analyzed to explore their correlation with N<sub>2</sub>O accumulation.

Across the treatment groups, key *nirK*, *nirS*, *norB*, and *nosZ* denitrifying bacterial species (Fig. 6g and h, and Fig. S9a and b) enriched in FS showed either statistically significant ( $p<0.05$ ) or insignificant but negative correlations with N<sub>2</sub>O emissions. In contrast, those enriched in BS were positively correlated with N<sub>2</sub>O accumulation. Notably, several key denitrifying species related to *Rhodanobacter*, such as *nirK*, *norB*, and *nosZ* based *Rhodanobacter sp.*, *nirK* and *norB* based *Rhodanobacter thiooxydans*, and *nirK* and *nosZ* based *Rhodanobacter glycinis*, were enriched only in the BS of NSC and BSB groups and exhibited a positive correlation with N<sub>2</sub>O emissions (Fig. 6g and h, and Fig. S9a).

On the other hand, key denitrifying species related to *Pseudomonas*, such as *nirS* based *Pseudomonadota bacterium* and *norB* and *nosZ* based *Pseudomonas sp.*, were enriched only in FS across different groups and showed a negative correlation with N<sub>2</sub>O emissions (Fig. 6g and h, and Fig. S9b). Similarly, species related to *Stutzerimonas*, such as key *nirS* based *Stutzerimonas nitrititolerans* (Fig. S9b) and *norB* based *Stutzerimonas degradans* (Fig. 6g), were enriched in the FS of the FSB group and were negatively correlated with N<sub>2</sub>O accumulation. Most importantly, several *nosZ* based key *Stutzerimonas* species, including *Stutzerimonas degradans*, *Stutzerimonas nitrititolerans*, and *Stutzerimonas sp.* (Fig. 6h), showed a significant negative correlation with N<sub>2</sub>O emissions and appeared as potential N<sub>2</sub>O reducing bacteria in the FS of FSB group.

#### Impact of recipient soil on denitrifying bacterial community

The PLSPM was employed to assess soil influences on denitrifying bacterial communities, specifically *nirK*, *nirS*, *norB*, and *nosZ*. As illustrated in Fig. 7 and Table S6, the interactions between soil environments, gene

abundances, diversity indices, and N<sub>2</sub>O emissions are evident.

In the *nirK* community model (Fig. 7a), soil positively impacts both the *nirK* community (path coefficient=0.97) and N<sub>2</sub>O emissions (path coefficient=0.94). Additionally, soil conditions influence *nirK* gene abundance (path coefficient=0.39) and diversity (path coefficient=0.27). In contrast, the *nirS* model (Fig. 7b) shows that soil type negatively influences *nirS* community structure (path coefficient = -0.91) and gene abundance (path coefficient = -0.82), with *nirS* gene abundance significantly negatively correlating with N<sub>2</sub>O emissions (path coefficient = -0.58).

For the *norB* community (Fig. 7c), soil exhibits a significant positive relation with community structure (path coefficient=0.99) but negatively impacts diversity (path coefficient = -0.62). The *norB* structure significantly positively correlates with N<sub>2</sub>O emissions (path coefficient=0.95). Lastly, in the *nosZ* model (Fig. 7d), significant negative effects of soil type on community structure (path coefficient = -0.91) and diversity (path coefficient = -0.68) are noted, while the *nosZ* structure negatively impacts N<sub>2</sub>O emissions (path coefficient = -0.86). Overall, the goodness-of-fit (GoF) values for the community models range from 0.60 to 0.71, indicating satisfactory fits.

## Discussion

### N<sub>2</sub>O accumulation pattern between two soils

Variations in soil biological and physicochemical properties significantly influence N<sub>2</sub>O fluxes in agroecosystems [1, 7, 10]. Similar to Wu et al., [9], our study found substantial differences in N<sub>2</sub>O accumulation between FS and BS, which can be attributed to their unique physicochemical characteristics, such as indigenous microbiome and diverse edaphic conditions. These differences are usually reported to lead to varied and often complex responses to N additions in soils [15]. While literature often highlights variations in carbon (C) and N contents as key factors influencing denitrification potential [51], our results suggest otherwise. Despite an equal supply of C and N and maintaining their native microbial communities, the N<sub>2</sub>O emission rate of BS was 6.5 times higher than that of FS (Fig. 1a, d). This observation indicates that differences in N<sub>2</sub>O accumulation between FS and BS are likely driven by more influential factors, such as their distinct denitrifying bacterial communities [9] and other physicochemical properties. These findings underscore the need for a deeper understanding of the interplay between soil characteristics and microbial communities to more accurately predict and manage N<sub>2</sub>O fluxes in agricultural systems.

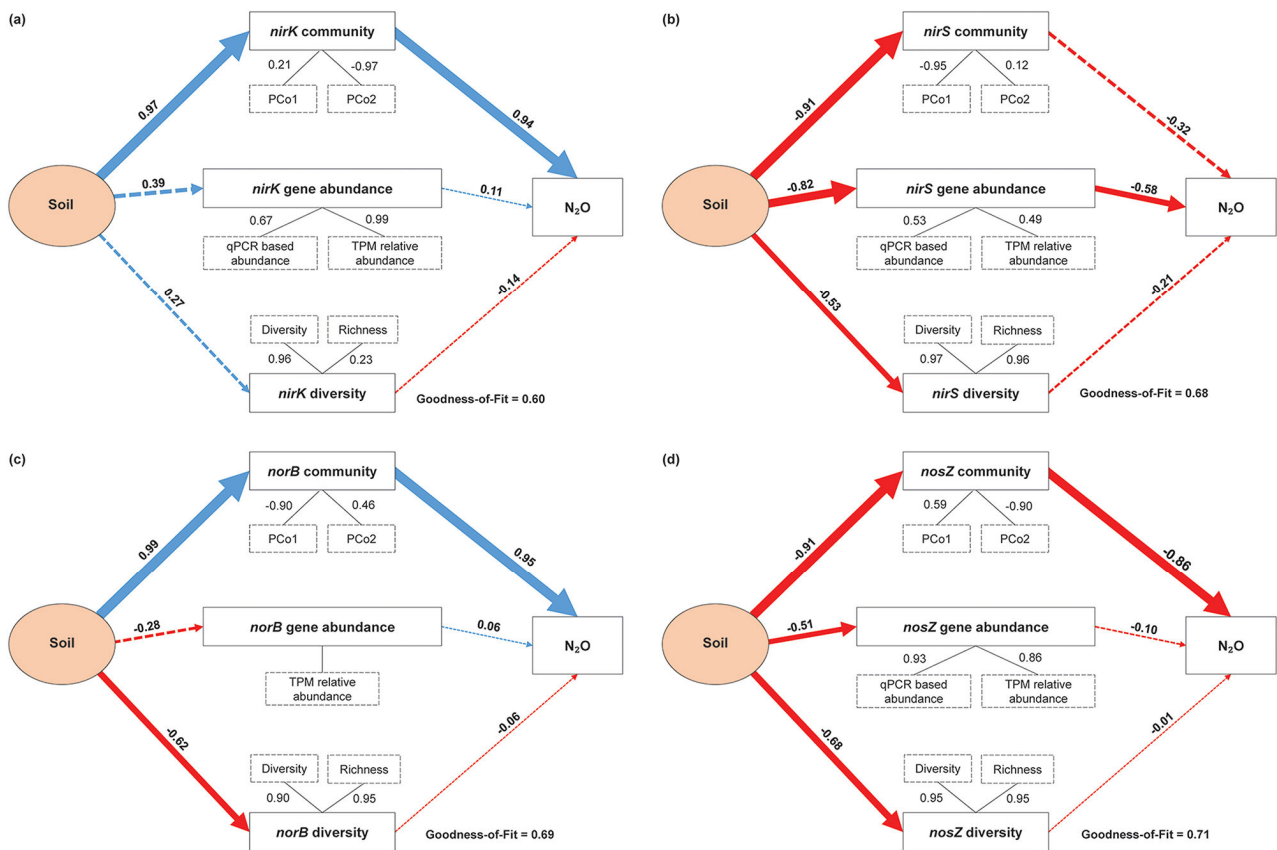


**Fig. 7** Effects of soil type on denitrifying community diversity and composition. Directed graphs of the PLSPM depicting the impact of soil conditions on the (a) *nirK*, (b) *nirS*, (c) *norB*, and (d) *nosZ* denitrifying communities. Each rectangular box represents an observed variable (i.e., measured) or a latent variable (i.e., constructs). Path coefficients are calculated after 1000 bootstraps and are reflected in the solid width of the arrows, with blue and red indicating positive and negative effects, respectively. The loadings for the community structure and diversity that create the latent variables are shown in the dashed rectangles. Dashed arrows indicate that coefficients did not differ significantly ( $p > 0.05$ ). The model is assessed using the GoF statistics

### Effects of extraction biases on the relevance of extracted bacteriomes to original soil

The cell extraction methods used can extract only a portion of soil cells [31], introducing potential biases in the composition and functioning of the extracted microbial community, such as differences in diversity [52] and N<sub>2</sub>O emission potential [53]. The functional relevance of extracted bacteriomes to their origin soils depends on how accurately they represent soil bacteriomes. Our findings showed high similarity between the composition of bacteriomes from parent soils and extracted cells, despite biases against certain taxa like Acidobacteria and Firmicutes (Fig. S2c, d), consistent with Highton et al. [33]. Despite these constraints, the conserved N<sub>2</sub>O accumulation patterns (Fig. S3) between soils and extracted bacteriomes indicate functional similarity. This underscores the importance of considering both microbial community composition and soil physicochemical properties when studying N<sub>2</sub>O emissions.

### N<sub>2</sub>O Accumulation responses

Several studies have highlighted the influence of soil physicochemical properties and environmental factors as key triggers for microbial-mediated N<sub>2</sub>O emissions from soils [7, 11–14]. In our study, BS consistently exhibited higher N<sub>2</sub>O accumulation, particularly in the NSC (6.50 times), FSB (21.74 times), and BSB (3.26 times) groups, and a significantly higher N<sub>2</sub>O/(N<sub>2</sub>O+N<sub>2</sub>) ratio compared to FS ( $p < 0.001$ ). The observed significant differences in N<sub>2</sub>O and N<sub>2</sub> accumulation dynamics between FS and BS across various treatment groups highlight the critical role of varying soil properties in these processes.

For the NSC group, the sustained increase in N<sub>2</sub>O production in both BS and FS suggests a stable enhancement in microbial activity or the denitrification process. In the FSB group, the dramatic late increase in N<sub>2</sub>O accumulation in BS indicates an accelerated denitrification process, triggering enhanced N<sub>2</sub>O production. The consistently lower and steady accumulation of N<sub>2</sub>O in FS compared to BS during the incubation period indicates a differential response of the FSB between FS and BS, likely due to variations in microbial community structure [16].

Similarly, the quicker and lower-level accumulation of N<sub>2</sub>O in FS of the BSB group compared to BS also points to divergent underlying denitrification processes contributing to N<sub>2</sub>O emissions.

These findings underscore that N<sub>2</sub>O accumulation is more strongly associated with soil environment rather than bacteriome type. The recipient soil-induced shifts in the denitrification process of the inoculated bacteriome might be influenced mainly by the variation in soil pH along with other properties. As pH can directly or indirectly affect the denitrification process and the denitrifying microbial community, either by inhibiting the assembly and activity of N<sub>2</sub>O reductase [12, 16] or by eliciting different responses from various microbial pathways to pH changes [54]. Acidic conditions are known to create an imbalance between N<sub>2</sub>O production and consumption, ultimately resulting in net N<sub>2</sub>O accumulation [12, 25, 55]. The acidic conditions of BS and the alkaline conditions of FS (Table 1) are likely significant factors contributing to the observed N<sub>2</sub>O accumulation patterns.

#### Effects on denitrifying functional genes

Our study supports the established correlation between N<sub>2</sub>O emissions in soils and denitrifying genes, notably *nirK* and *nosZ*, which have shown strong positive and negative correlations with potential N<sub>2</sub>O emissions [12, 55, 56]. Soils with high pH and clayey texture exhibit more robust denitrification potential compared to acidic and sandy soils owing to their ability to retain water and organic matter, creating more anaerobic microsites necessary for denitrification which create favourable conditions for denitrifying bacteria [57, 58]. Besides, the anoxic FS condition has been previously indicated as more favourable environment for the accelerated complete denitrification process [59].

Consistent with previous research [9], we observed higher relative abundances of *narG*, *nirK*, *nirS*, and *nosZ* in clayey and alkaline FS, indicating a more robust denitrification potential in these soils compared to sandy and acidic BS in the NSC. This trend was further substantiated in the FSB group, where the initial relative abundances of *narG* and *nirK* were significantly higher in FS. However, towards the end of the incubation, we observed a significant elevation in *nirK* abundance in BS, and higher abundances of *nirS*, *norB*, *norC*, and *nosZ* in FS, which suggest differential microbial adaptations and gene regulations in response to the conditions of the recipient soil. Notably, in the BSB group, the consistently higher *nirK* abundance in BS points to microbial adaptation favouring this gene under anoxic conditions.

The qPCR data (Fig. S5) corroborate our metagenomic findings (Fig. 2), reflecting similar trends in gene abundance. The *nirS* gene, known to be sensitive to soil variation such as pH [60], showed lower abundance in the

acidic BS conditions, particularly in the high-pH-adapted bacteriome of the FSB group. Conversely, the abundance of *nirK*, which is positively correlated with N<sub>2</sub>O emissions across various soils [55, 61], was higher in BS, aligning with its higher N<sub>2</sub>O emissions. Furthermore, higher *nirK/nosZ* ratios in BS suggest a shift towards incomplete denitrification processes, while higher *nirS/nosZ* ratios in FS indicate a balance favouring a complete denitrification pathway. A study by Liu et al. [62] identified a negative correlation between N<sub>2</sub>O flux and the copy numbers of *nirS* and *nosZ* genes. They also found that an increase in the numbers of these genes accelerated the reduction of N<sub>2</sub>O to N<sub>2</sub>.

These findings highlight significant variations in denitrification gene abundances for the same bacteriome between FS and BS conditions, underscoring the influence of soil properties on microbial community structure and denitrification potential.

#### Divergent bacterial communities caused by recipient soils

Microbial diversity and community composition are crucial for system stability and microbial functioning [26, 27, 63]. Specialized functions such as denitrification, nitrification, and pesticide mineralization are performed by specific microbial groups and are sensitive to changes in microbial composition and diversity [63, 64].

In this study, we observed variations in microbial community composition and diversity between FS and BS across different treatment groups, highlighting the complex dynamics of microbial adaptation to the exposed environmental conditions [65]. Previous studies have shown that inoculated microbial communities in sterile soils often lose taxonomic diversity compared to their origin soils [66, 67]. Consistent with these findings, the drastic decrease over time in observed features and Shannon index values in both FSB and BSB groups, compared to the NSC group, underscores the profound sensitivity of the inoculated microbiomes to sterile anoxic soil conditions. In contrast, the significant increase in diversity indices in FS and the decrease in BS over time within the NSC group indicate the stability and robustness of FS microbial communities in an anoxic soil environment compared to BS.

Shifts in taxonomic composition over time reveal distinct patterns of microbial succession. The initial dominance and subsequent decline of Actinomycetota and Acidobacteriota in the FSB and BSB groups reflect changing microbial dynamics. Microbial succession in response to changes in the soil environment is a dynamic process where microbial community composition and functioning shift to promote a more resilient soil ecosystem [68]. However, the microbial inoculums can also significantly influence community composition [69]. This is evident from the notable increase in Pseudomonadota

and Bacillota in the FSB group, and the rise in Bacteroidota and Gemmatimonadota in the BSB group, highlighting the differential enrichment of specific phyla driven by distinct microbial inoculums.

The enrichment of genera such as *Pseudomonas*, *Clostridium*, and *Bacillus* across groups suggests that these genera play key roles in microbial adaptation to anoxic conditions and are integral to nutrient cycling and energy flow in anoxic environments [70–72]. Additionally, the enrichment of specific genera like *Azotobacter*, *Enterobacter*, *Klebsiella*, and *Kosakonia* in FS and *Achromobacter* in BS demonstrates specific soil dependent responses of microbial communities. In short, the significant dynamic shifts in microbial populations and the enrichment of specific taxa highlight the complex interplay between microbial communities and their environments.

#### Linkage between shifts in Denitrifying guilds and N<sub>2</sub>O Emission

In soils, denitrifying guilds, functional groups of bacteria harboring specific denitrification genes, play a crucial role in regulating the balance between N<sub>2</sub>O production and consumption, ultimately influencing N<sub>2</sub>O fluxes [19, 63, 73]. Our study observed significant shifts in the taxonomic composition of denitrifying bacterial communities between FS and BS across various treatment groups, underscoring the strong influence of soil properties on denitrification potential and N<sub>2</sub>O emissions.

Previous research has shown that soil properties anchor distinct *nirK*- and *nirS*-based denitrifier communities [74–76]. Our study found few *nirS*-based denitrifiers, mainly in FS, suggesting these denitrifiers are more sensitive to changes such as soil type, moisture, and pH [60, 76]. In the NSC group, *Ramlibacter*, a genus with a comprehensive set of denitrification genes (*narG*, *nirK*, *nirS*, *norB*, and *nosZ*), was more enriched in FS, indicating that FS conditions favor higher denitrification potential. This trend was consistent across groups, with FS generally supporting a more diverse and active denitrifying community than BS. Notably, in the FSB group, complete denitrifiers with *nirS*, *norB*, and *nosZ* genes, such as *Pseudomonas* and *Stutzerimonas*, were significantly enriched in FS. These genera negatively correlated with N<sub>2</sub>O emissions, indicating their role in reducing N<sub>2</sub>O accumulation through complete denitrification pathways. Previous studies have reported the N<sub>2</sub>O reducing potential of *Pseudomonas* and *Stutzerimonas* [71, 77–79], highlighting their significance as complete denitrifiers.

For example, inoculating two *Stutzerimonas stutzeri* strains, NRCB010 and NRCB025, promoted tomato growth and reduced N<sub>2</sub>O emissions in agricultural soils, with NRCB010 decreasing emissions by 38.7–52.2% and NRCB025 by 76.6% [77]. Another study noted the high

potential of the NRCB010 strain (previously known as *Pseudomonas stutzeri*) for improving crop productivity and mitigating N<sub>2</sub>O emissions in agricultural soils [79]. Furthermore, a recent study by Zhang et al. [80] identified denitrifying microorganisms in the deep vadose zone of an intensive agricultural area in China, revealing high denitrification activity in two complete denitrifiers belonging to the genus *Pseudomonas*. These findings suggest that bacteria of these genera may play a central role in the denitrification process in FS. Further, enrichment of potential *nosZ*-containing bacteria could help eliminate N<sub>2</sub>O emissions [19, 81]. Our study identified significant enrichment of *nosZ*-containing genera, including *Aromatoleum*, *Ramlibacter*, *Pseudomonas*, and *Stutzerimonas*, in FS across groups. The delay in the onset of denitrification in BS of the FSB group, with extensive N<sub>2</sub>O accumulation, might be attributed to the loss of such potential denitrifiers.

Conversely, the relative abundance of *nirK* genes in the FSB and BSB groups was higher in BS than in FS, potentially facilitating increased N<sub>2</sub>O generation in BS. BS also showed higher enrichment of *nirK*-containing taxa such as *Paenibacillus* and *Geobacillus*. Additionally, *Rhodanobacter*, containing both *nirK* and *norB* genes, emerged as the dominant denitrifier in BS, with a strong positive correlation between these biomarker species, particularly *Rhodanobacter* and *Achromobacter*, and N<sub>2</sub>O accumulation. Previous studies identified *Rhodanobacter* as a prevalent denitrifier in agricultural BS [9, 82]. Specifically, 18 *Rhodanobacter* isolates from Wu et al. [9] and three from Lycus et al. [8] demonstrated significant roles in N<sub>2</sub>O accumulation due to their truncated denitrification genes and lack of N<sub>2</sub>O reduction capacity. *Achromobacter*, also containing the *nirK* gene [83], has been shown to enhance N<sub>2</sub>O spillover [84]. Thus, the enrichment of *nirK*- and *norB*-containing *Rhodanobacter* and *Achromobacter* as dominant denitrifiers may impede the complete denitrification process, potentially leading to increased N<sub>2</sub>O emissions in BS across the treatment groups. However, in the FS of the BSB group, where the relative abundance of *Rhodanobacter* dropped significantly, this effect might be mitigated.

Alpha and beta diversity analyses further underscored the structural and compositional differences in denitrifying communities between FS and BS. PCoA plots indicate a significant temporal divergence in the denitrifying communities between the FS and BS across groups. For the inoculant groups, the denitrifying communities of the same inoculated bacteriome were significantly divergent between FS and BS over time and were structurally more related to recipient soil microbiome instead of the inoculum. Our observations align with findings from a previous study where the soil communities possessed functional and taxonomical structures more related to

the recipient sterile soils after inoculation and incubation [85]. Further, FS showed significant increases in Shannon index and observed features across most groups, suggesting that FS promotes a more diverse and complex microbial community. This increased diversity may enhance the overall functional resilience and efficiency of the denitrification process, potentially reducing N<sub>2</sub>O emissions. In contrast, the FSB group's pattern of increased diversity in FS but decreased diversity in BS highlights the varying impacts of recipient soil on denitrifying microbial community dynamics. As microbial diversity is crucial for system stability and microbial functioning [27], the decline in diversity in BS could lead to a less stable and low efficiency in denitrification process, contributing to higher N<sub>2</sub>O emissions. In short, similar to literature where the composition of *nirK*, *nirS*, and *nosZ*-based denitrifiers influences the enzymatic activity of the denitrification process [74, 75, 86]. Distinct *nirK* and *norB*, and *nirS* and *nosZ* based denitrifiers appeared as important groups for the differential N<sub>2</sub>O accumulation patterns in our study.

PLSPM analysis provided a holistic view of the interactions between soil properties, denitrifying bacterial communities, gene abundances, and N<sub>2</sub>O emissions. The significant positive effect of soil condition on *nirK* and *norB* communities and their correlation with increased N<sub>2</sub>O emissions highlights the role of these genes in N<sub>2</sub>O production. Conversely, the negative influence of soil condition on *nirS* and *nosZ* communities, along with their negative correlations with N<sub>2</sub>O emissions, suggests that enhancing the abundance and activity of these communities could be a strategy for reducing N<sub>2</sub>O emissions.

In summary, our study highlights the intricate relationships between soil properties, denitrifying bacterial community composition, and N<sub>2</sub>O emissions. Our results suggest that the recipient soil properties alter the denitrifier composition of the inoculated bacteriomes, ultimately affecting the activities of denitrifying enzymes and resulting in different patterns of N<sub>2</sub>O emission.

## Conclusions

This study reveals the crucial role of soil properties as distal drivers in shaping proximal denitrifying bacterial communities and their influence on N<sub>2</sub>O emissions. The variation in N<sub>2</sub>O accumulation between FS and BS, even when inoculated with the same microbiome, highlights the impact of recipient soil characteristics on microbial dynamics. BS favoured *nirK*-based denitrifiers like *Rhodanobacter*, leading to incomplete denitrification and higher N<sub>2</sub>O emissions, whereas FS supported a more diverse range of denitrifiers, such as *Pseudomonas* and *Stutzerimonas*, promoting complete denitrification and lower emissions. These findings underscore the importance of soil properties in modulating microbial structure

and function, which is vital for strategies to optimize denitrification and reduce N<sub>2</sub>O emissions in agricultural systems. Future research should explore manipulating soil microbial communities with targeted denitrifiers and applying multi-omics approaches to better understand microbial functions. Expanding the range of soil samples from diverse locations would also strengthen the generalizability of these conclusions, offering a basis for targeted interventions that enhance sustainable agricultural practices and contribute to greenhouse gas mitigation.

## Supplementary Information

The online version contains supplementary material available at <https://doi.org/10.1186/s40793-024-00643-9>.

Supplementary Material 1

## Acknowledgements

This work was supported by the National Natural Science Foundation of China (NSFC project 31971526), and the National Key Research and Development Program of China (2017YFD0200102).

## Author contributions

Saira Bano: conceptualization, methodology, and writing original draft. Qiaoyu Wu: methodology and robot experiment. Siyu Yu: methodology and QPCR experiment. Xinhui Wang: methodology and robot experiment. Xiaojun Zhang: conceptualization, investigation, writing-review and editing, supervision, and funding acquisition.

## Data availability

The raw Illumina sequence data of the 16S rRNA gene V3-V4 region and metagenomic sequences is available in the GenBank Sequence Read Archive (SRA) database of the National Center for Biotechnology Information (NCBI) under BioProject accession number PRJNA992239 and PRJNA1138288, respectively.

## Declarations

### Competing interests

The authors declare no competing interests.

Received: 12 August 2024 / Accepted: 14 November 2024

Published online: 21 November 2024

## References

1. Tian H, Xu R, Canadell JG, Thompson RL, Winiwarter W, Suntharalingam P, Davidson EA, Ciais P, Jackson RB, Janssens-Maenhout G, et al. A comprehensive quantification of global nitrous oxide sources and sinks. *Nature*. 2020;586(7828):248–56.
2. Masson-Delmotte V, Zhai P, Pirani A, Connors SL, Péan C, Berger S, Caud N, Chen Y, Goldfarb L, Gomis MI, Huang M, Leitzell K, Lonnoy E, Matthews JBR, Maycock TK, Waterfield T, Yelekçi O, Yu R, Zhou B, editors. *Climate Change 2021: the physical science basis. Contribution of Working Group I to the Sixth Assessment Report of the Intergovernmental Panel on Climate Change*. Cambridge, United Kingdom: Cambridge University Press; 2021.
3. López-Aizpún M, Horrocks CA, Charteris AF, Marsden KA, Ciganda VS, Evans JR, Chadwick DR, Cárdenas LM. Meta-analysis of global livestock urine-derived nitrous oxide emissions from agricultural soils. *Glob Change Biol*. 2020;26(4):2002–13.
4. Kool DM, Dolfing J, Wrage N, Van Groenigen JW. Nitrifier denitrification as a distinct and significant source of nitrous oxide from soil. *Soil Biol Biochem*. 2011;43(1):174–8.

5. Firestone MK, Davidson EA. Microbiological basis of NO and N<sub>2</sub>O production and consumption in soil. *Exch Trace Gases between Terr Ecosyst Atmos*. 1989;47:7–21.
6. Liu B, Zhang X, Bakken LR, Snipen L, Frostegård Å. Rapid Succession of actively transcribing denitrifier populations in Agricultural Soil during an anoxic spell. *Front Microbiol* 2019, 9.
7. Gao J, Xie Y, Jin H, Liu Y, Bai X, Ma D, Zhu Y, Wang C, Guo T. Nitrous Oxide Emission and Denitrifier abundance in two agricultural soils amended with crop residues and urea in the North China Plain. *PLoS ONE*. 2016;11(5):e0154773.
8. Lycus P, Lovise Bøthun K, Bergaust L, Peele Shapleigh J, Reier Bakken L, Frostegård Å. Phenotypic and genotypic richness of denitrifiers revealed by a novel isolation strategy. *ISME J*. 2017;11(10):2219–32.
9. Wu Q, Ji M, Yu S, Li J, Wu X, Ju X, Liu B, Zhang X. Distinct denitrifying phenotypes of predominant Bacteria modulate Nitrous Oxide Metabolism in two typical Cropland soils. *Microbial Ecology*; 2022.
10. Yang L, Zhang X, Ju X. Linkage between N<sub>2</sub>O emission and functional gene abundance in an intensively managed calcareous fluvo-aquic soil. *Sci Rep*. 2017;7(1):43283.
11. Girvan MS, Bullimore J, Pretty JN, Osborn AM, Ball AS. Soil type is the primary determinant of the composition of the total and active bacterial communities in Arable soils. *Appl Environ Microbiol*. 2003;69(3):1800–9.
12. Liu B, Mørkved PT, Frostegård Å, Bakken LR. Denitrification gene pools, transcription and kinetics of NO, N<sub>2</sub>O and N<sub>2</sub> production as affected by soil pH. *FEMS Microbiol Ecol*. 2010;72(3):407–17.
13. Lin S, Hernandez-Ramirez G. Nitrous oxide emissions from manured soils as a function of various nitrification inhibitor rates and soil moisture contents. *Sci Total Environ*. 2020;738:139669.
14. Chen H, Zeng L, Wang D, Zhou Y, Yang X. Exploring the linkage between free nitrous acid accumulation and nitrous oxide emissions in a novel static/oxic/anoxic process. *Bioresour Technol*. 2020;304:123011.
15. Ullah S, He P, Ai C, Zhao S, Ding W, Song D, Zhang J, Huang S, Abbas T, Zhou W. How Do Soil Bacterial Diversity and Community Composition Respond under Recommended and Conventional Nitrogen Fertilization Regimes? *Microorganisms* 2020, 8(8):1193.
16. Bakken LR, Bergaust L, Liu B, Frostegård Å. Regulation of denitrification at the cellular level: a clue to the understanding of N < sub > 2 O emissions from soils. *Philosophical Trans Royal Soc B: Biol Sci*. 2012;367(1593):1226–34.
17. Philippot L, Chenu C, Kappler A, Rillig MC, Fierer N. The interplay between microbial communities and soil properties. *Nat Rev Microbiol* 2023.
18. Xiao X, Xie G, Yang Z, He N, Yang D, Liu M. Variation in abundance, diversity, and composition of nirK and nirS containing denitrifying bacterial communities in a red paddy soil as affected by combined organic-chemical fertilization. *Appl Soil Ecol*. 2021;166:104001.
19. Ji M, Tian H, Wu X, Li J, Zhu Y, Wu G, Xu T, Wang J, Zhang X. Enhanced N<sub>2</sub>O emission rate in field soil undergoing conventional intensive fertilization is attributed to the shifts of denitrifying guilds. *Pedosphere*. 2021;31(1):145–56.
20. Tubiello FN, Salvatore M, Córdor Golec RD, Ferrara A, Rossi S, Biancalani R, Federici S, Jacobs H, Flammini A. Agriculture, forestry and other land use emissions by sources and removals by sinks. *Rome, Italy* 2014.
21. Lejpnik M, Su Y, Ye X. The Main Agricultural Regions of China and the U.S. In: *A Comparative Geography of China and the US*. Edited by Hartmann R, Wang Ja, Ye T. Dordrecht: Springer Netherlands; 2014: 309–351.
22. Kang S, Eltahir EAB. North China Plain threatened by deadly heatwaves due to climate change and irrigation. *Nat Commun*. 2018;9(1):2894.
23. Ju X-T, Xing G-X, Chen X-P, Zhang S-L, Zhang L-J, Liu X-J, Cui Z-L, Yin B, Christie P, Zhu Z-L et al. Reducing environmental risk by improving N management in intensive Chinese agricultural systems. *Proceedings of the National Academy of Sciences* 2009, 106(9):3041–3046.
24. Lu X, Ye X, Zhou M, Zhao Y, Weng H, Kong H, Li K, Gao M, Zheng B, Lin J, et al. The underappreciated role of agricultural soil nitrogen oxide emissions in ozone pollution regulation in North China. *Nat Commun*. 2021;12(1):5021.
25. Zhu G, Song X, Ju X, Zhang J, Müller C, Sylvester-Bradley R, Thorman RE, Bingham I, Rees RM. Gross N transformation rates and related N<sub>2</sub>O emissions in Chinese and UK agricultural soils. *Sci Total Environ*. 2019;666:176–86.
26. Jansson JK, Hofmockel KS. Soil microbiomes and climate change. *Nat Rev Microbiol*. 2020;18(1):35–46.
27. Hartmann M, Six J. Soil structure and microbiome functions in agroecosystems. *Nat Reviews Earth Environ*. 2023;4(1):4–18.
28. Prosser JL. Dispersing misconceptions and identifying opportunities for the use of omics' in soil microbial ecology. *Nat Rev Microbiol*. 2015;13(7):439–46.
29. Roco CA, Dörsch P, Booth JG, Pepe-Ranney C, Groffman PM, Fahey TJ, Yavitt JB, Shapleigh JP. Using metagenomics to reveal landscape scale patterns of denitrifiers in a montane forest ecosystem. *Soil Biol Biochem*. 2019;138:107585.
30. Govindasamy P, Mahawer SK, Mowrer J, Bagavathiannan M, Prasad M, Ramakrishnan S, Halli HM, Kumar S, Chandra A. Comparison of low-cost methods for Soil Water Holding Capacity. *Commun Soil Sci Plant Anal*. 2023;54(2):287–96.
31. Lindahl V, Bakken LR. Evaluation of methods for extraction of bacteria from soil. *FEMS Microbiol Ecol*. 1995;16(2):135–42.
32. Barra Caracciolo A, Grenni P, Cupo C, Rossetti S. In situ analysis of native microbial communities in complex samples with high particulate loads. *FEMS Microbiol Lett*. 2005;253(1):55–8.
33. Highton MP, Bakken LR, Dörsch P, Tobias-Hunefeldt S, Molstad L, Morales SE. Soil water extract and bacteriome determine N<sub>2</sub>O emission potential in soils. *Biol Fertil Soils*. 2023;59(2):217–32.
34. Molstad L, Dörsch P, Bakken LR. Robotized incubation system for monitoring gases (O<sub>2</sub>, NO, N<sub>2</sub>O N<sub>2</sub>) in denitrifying cultures. *J Microbiol Methods*. 2007;71(3):202–11.
35. Wu X, Li J, Ji M, Wu Q, Wu X, Ma Y, Sui W, Zhao L, Zhang X. Non-synchronous structural and functional dynamics during the Coalescence of two distinct soil bacterial communities. *Front Microbiol* 2019, 10.
36. Caporaso JG, Kuczynski J, Stombaugh J, Bittinger K, Bushman FD, Costello EK, Fierer N, Peña AG, Goodrich JK, Gordon JL. QIIME allows analysis of high-throughput community sequencing data. *Nat Methods*. 2010;7(5):335–6.
37. Callahan BJ, McMurdie PJ, Rosen MJ, Han AW, Johnson AJA, Holmes SP. DADA2: high-resolution sample inference from Illumina amplicon data. *Nat Methods*. 2016;13(7):581–3.
38. Price MN, Dehal PS, Arkin AP. FastTree: computing large minimum evolution trees with profiles instead of a distance matrix. *Mol Biol Evol*. 2009;26(7):1641–50.
39. Chen S, Zhou Y, Chen Y, Gu J. Fastp: an ultra-fast all-in-one FASTQ preprocessor. *Bioinformatics*. 2018;34(17):i884–90.
40. Li D, Liu CM, Luo R, Sadakane K, Lam TW. MEGAHIT: an ultra-fast single-node solution for large and complex metagenomics assembly via succinct de bruijn graph. *Bioinformatics*. 2015;31(10):1674–6.
41. Hyatt D, Chen G-L, LoCascio PF, Land ML, Larimer FW, Hauser LJ. Prodigal: prokaryotic gene recognition and translation initiation site identification. *BMC Bioinformatics*. 2010;11(1):119.
42. Steinegger M, Söding J. MMseqs2 enables sensitive protein sequence searching for the analysis of massive data sets. *Nat Biotechnol*. 2017;35(11):1026–8.
43. Buchfrnk B, Xie C, Huson DH. Fast and sensitive protein alignment using DIAMOND. *Nat Methods*. 2015;12(1):59–60.
44. Xie C, Mao X, Huang J, Ding Y, Wu J, Dong S, Kong L, Gao G, Li CY, Wei L. KOBAS 2.0: a web server for annotation and identification of enriched pathways and diseases. *Nucleic Acids Res*. 2011;39(Web Server issue):W316–322.
45. Seyler LM, Trembath-Reichert E, Tully BJ, Huber JA. Time-series transcriptomics from cold, oxic seafloor crustal fluids reveals a motile, mixotrophic microbial community. *ISME J*. 2021;15(4):1192–206.
46. Robinson MD, McCarthy DJ, Smyth GK. edgeR: a Bioconductor package for differential expression analysis of digital gene expression data. *Bioinformatics*. 2009;26(1):139–40.
47. Dixon P. VEGAN, a package of R functions for community ecology. *J Veg Sci*. 2003;14(6):927–30.
48. Segata N, Izard J, Waldron L, Gevers D, Miropolsky L, Garrett WS, Huttenhower C. Metagenomic biomarker discovery and explanation. *Genome Biol*. 2011;12(6):R60.
49. Sanchez G, Trinchera L, Sanchez MG, FactoMineR S. Package 'plsppm'. *Citeseer: State College, PA, USA* 2013.
50. Team RC. R: a Language and Environment for Statistical Computing. In: Vienna. Austria: R Foundation for Statistical Computing; 2010.
51. Wu X, Liu G, Butterbach-Bahl K, Fu B, Zheng X, Brüggemann N. Effects of land cover and soil properties on denitrification potential in soils of two semi-arid grasslands in Inner Mongolia, China. *J Arid Environ*. 2013;92:98–101.
52. Holmgaard PN, Norman A, Hede SC, Poulsen PHB, Al-Soud WA, Hansen LH, Sørensen SJ. Bias in bacterial diversity as a result of Nycodenz extraction from bulk soil. *Soil Biol Biochem*. 2011;43(10):2152–9.
53. Nadeem S, Almås ÅR, Dörsch P, Bakken LR. Sequential extraction of denitrifying organisms from soils; strongly attached cells produce less N<sub>2</sub>O than loosely attached cells. *Soil Biol Biochem*. 2013;67:62–9.
54. Richardson D, Felgate H, Watmough N, Thomson A, Baggs E. Mitigating release of the potent greenhouse gas N<sub>2</sub>O from the nitrogen cycle—could enzymic regulation hold the key? *Trends Biotechnol*. 2009;27(7):388–97.

55. Li S, Song L, Jin Y, Liu S, Shen Q, Zou J. Linking N<sub>2</sub>O emission from biochar-amended composting process to the abundance of denitrifier (nirK and nosZ) bacteria community. *Amb Express*. 2016;6(1):1–9.
56. Morales SE, Cosart T, Holben WE. Bacterial gene abundances as indicators of greenhouse gas emission in soils. *ISME J*. 2010;4(6):799–808.
57. Gaillard R, Duval BD, Osterholz WR, Kucharik CJ. Simulated effects of soil texture on nitrous oxide emission factors from corn and soybean agroecosystems in Wisconsin. *J Environ Qual*. 2016;45(5):1540–8.
58. Domeignoz-Horta LA, Philippot L, Peyrard C, Bru D, Breuil MC, Bizouard F, Justes E, Mary B, Léonard J, Spor A. Peaks of in situ N<sub>2</sub>O emissions are influenced by N<sub>2</sub>O-producing and reducing microbial communities across arable soils. *Glob Change Biol*. 2018;24(1):360–70.
59. Yang L, Zhu G, Ju X, Liu R. Oxygen concentrations regulate NO, N<sub>2</sub>O, and N<sub>2</sub> kinetics and nitrogen transformation in a fluvo-aquic soil using a robotized incubation system. *J Soils Sediments*. 2021;21(3):1337–47.
60. Sun H, Jiang S. A review on Nirs-type and nirK-type denitrifiers via a scientific approach coupled with case studies. *Environ Science: Processes Impacts*. 2022;24(2):221–32.
61. Wang N, Luo J-L, Juhasz AL, Li H-B, Yu J-G. Straw decreased N<sub>2</sub>O emissions from flooded paddy soils via altering denitrifying bacterial community compositions and soil organic carbon fractions. *FEMS Microbiol Ecol* 2020, 96(5).
62. Liu X, Tang Z, Zhang Q, Kong W. The contrasting effects of biochar and straw on N<sub>2</sub>O emissions in the maize season in intensively farmed soil. *Environ Sci Pollut Res*. 2021;28(23):29806–19.
63. Kuypers MMM, Marchant HK, Kartal B. The microbial nitrogen-cycling network. *Nat Rev Microbiol*. 2018;16(5):263–76.
64. Hall EK, Bernhardt ES, Bier RL, Bradford MA, Boot CM, Cotner JB, del Giorgio PA, Evans SE, Graham EB, Jones SE, et al. Understanding how microbiomes influence the systems they inhabit. *Nat Microbiol*. 2018;3(9):977–82.
65. Wani AK, Akhtar N, Sher F, Navarrete AA, Américo-Pinheiro JHP. Microbial adaptation to different environmental conditions: molecular perspective of evolved genetic and cellular systems. *Arch Microbiol*. 2022;204(2):144.
66. Chen Q-L, Ding J, Zhu Y-G, He J-Z, Hu H-W. Soil bacterial taxonomic diversity is critical to maintaining the plant productivity. *Environ Int*. 2020;140:105766.
67. Doering T, Wall M, Putschim L, Rattanawongwan T, Schroeder R, Hentschel U, Roik A. Towards enhancing coral heat tolerance: a microbiome transplantation treatment using inoculations of homogenized coral tissues. *Microbiome*. 2021;9(1):102.
68. Fierer N, Jackson RB. The diversity and biogeography of soil bacterial communities. *Proceedings of the National Academy of Sciences* 2006, 103(3):626–631.
69. van der Heijden MGA, Hartmann M. Networking in the Plant Microbiome. *PLoS Biol*. 2016;14(2):e1002378.
70. Muyzer G, Stams AJM. The ecology and biotechnology of sulphate-reducing bacteria. *Nat Rev Microbiol*. 2008;6(6):441–54.
71. Zumft WG. Cell biology and molecular basis of denitrification. *Microbiol Mol Biol Rev*. 1997;61(4):533–616.
72. Philippot L, Hallin S, Schlöter M. Ecology of denitrifying prokaryotes in agricultural soil. *Adv Agron*. 2007;96:249–305.
73. Cavigelli MA, Robertson GP. Role of denitrifier diversity in rates of nitrous oxide consumption in a terrestrial ecosystem. *Soil Biol Biochem*. 2001;33(3):297–310.
74. Braker G, Matthies D, Hannig M, Brandt FB, Brenzinger K, Gröngröft A. Impact of Land Use Management and Soil properties on Denitrifier communities of Namibian savannas. *Microb Ecol*. 2015;70(4):981–92.
75. Jin W, Cao W, Liang F, Wen Y, Wang F, Dong Z, Song H. Water management impact on denitrifier community and denitrification activity in a paddy soil at different growth stages of rice. *Agric Water Manage*. 2020;241:106354.
76. Qin H, Xing X, Tang Y, Zhu B, Wei X, Chen X, Liu Y. Soil moisture and activity of nitrite- and nitrous oxide-reducing microbes enhanced nitrous oxide emissions in fallow paddy soils. *Biol Fertil Soils*. 2020;56(1):53–67.
77. *Microbiology Spectrum* 2024, 12(5):e00186-00124.
78. Jin Y, Liu D, Xiong W, Wu Z, Xiao G, Wang S, Su H. Enhancing nitrogen removal performance using immobilized aerobic denitrifying bacteria by modified polyvinyl alcohol/sodium alginate (PVA/SA). *Chemosphere*. 2024;357:141954.
79. Zhang H, Hu C, Li L, Lei P, Shen W, Xu H, Gao N. Effect of n-hexadecanoic acid on N<sub>2</sub>O emissions from vegetable soil and its synergism with *Pseudomonas stutzeri* NRCB010. *Appl Soil Ecol*. 2024;199:105410.
80. Zhang L, Zhao H, Qin S, Hu C, Shen Y, Qu B, Bai Y, Liu B. Genome-resolved metagenomics and denitrifying strain isolation reveal New insights into Microbial Denitrification in the Deep Vadose Zone. *Environ Sci Technol*. 2024;58(5):2323–34.
81. Hallin S, Philippot L, Löffler FE, Sanford RA, Jones CM. Genomics and Ecology of Novel N<sub>2</sub>O-Reducing microorganisms. *Trends Microbiol*. 2018;26(1):43–55.
82. Hu X, Liu J, Wei D, Zhu P, Cui Xa, Zhou B, Chen X, Jin J, Liu X, Wang G. Chronic effects of different fertilization regimes on Nirs-type denitrifier communities across the black soil region of Northeast China. *Pedosphere*. 2020;30(1):73–86.
83. Kou Y, Liu Y, Li J, Li C, Tu B, Yao M, Li X. Patterns and Drivers of nirK-Type and nirS-Type Denitrifier Community Assembly along an Elevation Gradient. *mSystems* 2021, 6(6):e0066721.
84. Dai X, Wang X, Gu J, Song Z, Guo H, Shi M, Li H. Mechanism associated with the positive effect of nanocellulose on nitrogen retention in a manure composting system. *J Environ Manage*. 2022;316:115308.
85. Delmont TO, Francioli D, Jacquesson S, Laoudi S, Mathieu A, Nesme J, Ceccherini MT, Nannipieri P, Simonet P, Vogel TM. Microbial community development and unseen diversity recovery in inoculated sterile soil. *Biol Fertil Soils*. 2014;50(7):1069–76.
86. Wan Z, Wang L, Huang G, Rasul F, Awan MI, Cui H, Liu K, Yu X, Tang H, Wang S, et al. nirS and nosZII bacterial denitrifiers as well as fungal denitrifiers are coupled with N<sub>2</sub>O emissions in long-term fertilized soils. *Sci Total Environ*. 2023;897:165426.

## Publisher's note

Springer Nature remains neutral with regard to jurisdictional claims in published maps and institutional affiliations.